

1 **Nitrogen speciation in various types of aerosols in**
2 **spring over the northwestern Pacific Ocean**

3 **L. Luo¹, X. H. Yao², H. W. Gao², S. C. Hsu³, J. W. Li⁴, S. J. Kao^{1,*}**

4 [1]{State Key Laboratory of Marine Environmental Science, Xiamen University,
5 Xiamen 361102, China}

6 [2]{Key laboratory of Marine Environmental Science and Ecology, Ministry of
7 Education, Ocean University of China, Qingdao 266100, China}

8 [3]{Research Center for Environmental Changes, Academia Sinica, Taipei, Taiwan}

9 [4]{Key Laboratory of Regional Climate-Environment for Temperate East Asia,
10 Institute of Atmospheric Physics, Chinese Academy of Sciences, Beijing 100029,
11 China}

12 Correspondence to: S. J. Kao (sjkao@xmu.edu.cn)

13

14 **Abstract**

15 The cumulative atmospheric nitrogen deposition has been found to profoundly impact
16 the nutrient stoichiometry of the East China seas (ECSs) and the northwestern Pacific
17 Ocean (NWPO). In spite of the potential significance of dry deposition in those
18 regions, ship-board observations of atmospheric aerosols remain insufficient,
19 particularly regarding the compositions of water-soluble nitrogen species (nitrate,
20 ammonium and water-soluble organic nitrogen – WSON). We conducted a cruise
21 covering the ECSs and the NWPO during the spring of 2014 and observed three types
22 of atmospheric aerosols. Aluminum content, air mass backward trajectories, weather
23 conditions, and ion stoichiometry allowed us to discern dust aerosol patches and sea
24 fog modified aerosols (widespread over the ECSs) from background aerosols (open
25 ocean). Among the three types, sea fog modified aerosols contained the highest
26 concentrations of nitrate ($536 \pm 300 \text{ nmol N m}^{-3}$), ammonium ($442 \pm 194 \text{ nmol N m}^{-3}$)
27 and WSON ($147 \pm 171 \text{ nmol N m}^{-3}$); furthermore, ammonium and nitrate together

1 occupied ~ 65% of the molar fraction of total ions. The dust aerosols also contained
2 significant amounts of nitrate ($100 \pm 23 \text{ nmol N m}^{-3}$) and ammonium ($138 \pm 24 \text{ nmol N m}^{-3}$) which were obviously larger than those in the background aerosols (26 ± 32
4 for nitrate and $54 \pm 45 \text{ nmol N m}^{-3}$ for ammonium), yet, this was not the case for
5 WSON. It appeared that dust aerosols had less of a chance to contact WSON during
6 their transport. In the open ocean, we found that sea salt (e.g. Na^+ , Cl^- , Mg^{2+}), as
7 well as WSON, correlated positively with wind speed. Apparently, marine dissolved
8 organic nitrogen (DON) was emitted during breaking waves. Regardless of the
9 variable wind speeds from 0.8 to as high as 18 m s^{-1} , nitrate and ammonium, by
10 contrast, remained in narrow ranges implying that some supply and consumption
11 processes of nitrate and ammonium were required to maintain such a quasi-static
12 condition. Mean dry deposition of total dissolved nitrogen (TDN) for sea fog
13 modified aerosols ($1090 \pm 671 \mu\text{mol N m}^{-2} \text{ d}^{-1}$) was 5 times higher than that for dust
14 aerosols ($190 \pm 41.6 \mu\text{mol N m}^{-2} \text{ d}^{-1}$) and around 20 times higher than that for
15 background aerosols ($56.8 \pm 59.1 \mu\text{mol N m}^{-2} \text{ d}^{-1}$). Apparently, spring sea fog on the
16 ECSs played an important role in removing atmospheric reactive nitrogen from the
17 Chinese mainland and depositing it into the ECSs, thus effectively preventing its
18 seaward export to the NWPO.

19

20 1 Introduction

21 Anthropogenic reactive nitrogen (Nr) emissions have dramatically increased in the last
22 few decades owing to rapidly growing populations and industry (Galloway et al.,
23 2008). China is one of the largest producers and emitters of Nr in the world (Nr
24 emission of 12.18 Tg y^{-1} ; Reis et al., 2009). Inevitably, large amounts of Nr emanate
25 into the adjacent seas through various pathways. Through the atmosphere, annual
26 nitrogen depositions into the east China seas (ECSs; the Yellow Sea and East China
27 Sea) had been reported to be the same order of magnitude carried by the Yangtze
28 River discharge (Nakamura et al., 2005; Zhang et al., 2007). Besides observational
29 data, global models revealed that both of the Chinese marginal seas and the

1 northwestern Pacific Ocean (NWPO) are under the atmospheric influence of the Asian
2 continent, which supplied significant amounts of anthropogenic Nr (Duce et al., 2008)
3 and terrigenous materials (Jickells et al., 2005). The cumulative effect of atmospheric
4 input in the past decades even altered the nutrient stoichiometry on a regional scale,
5 including the Chinese marginal seas and the North Pacific Ocean (T. W. Kim et al.,
6 2011; I. N. Kim et al., 2014).

7 To better constrain atmospheric deposition of Nr into the ocean over large spatial
8 and temporal scales, modeling the transport and deposition of air pollutants is
9 essential. Models of atmospheric nitrogen deposition include abundant parameters,
10 such as local emission densities, particle size, deposition velocity, chemical processes
11 and meteorological conditions (Liu et al., 2005; Guenther et al., 2006; Kanakidou et
12 al., 2012). However, model accuracy strongly relies on the validation by observational
13 data. Unfortunately, ship-board observations, particularly for an offshore gradient
14 from marginal seas to the open sea, are still limited.

15 In the marginal seas of China, dust and fog storms are two common intermittent
16 weather events during the transition period from a cold to a warm season (Sun et al.,
17 2001; Zhang et al., 2009). Dust aerosols may serve as a carrier bringing significant
18 amounts of terrigenous and anthropogenic fingerprints including trace elements (Duce
19 et al., 1980) and Nr (Chen and Chen, 2008) from inland into the open sea via
20 long-range transport. By contrast, sea fog is relatively stagnant and restricted on a
21 spatial scale. Fog is the intermediate stage between precipitation and aerosol. Fog
22 forms by the activation of particulate with subsequent growth and incorporation of
23 other gases and particles (Cape et al., 2011). Fog droplets are smaller in size when
24 compared to rain drops; however, concentrations of water-soluble species in fog water
25 were not necessarily higher or lower than those of precipitation because of
26 complicated chemical processes (Sasakawa et al., 2002; Watanabe et al., 2006; Jung et
27 al., 2013). Inland fog chemistry was well studied and its impacts on terrestrial
28 ecosystems were highlighted (Chang et al., 2002; Lange et al., 2003). Researchers
29 even designed experiments to investigate the differences in aerosol chemistry for pre-

1 and post- fog formation periods to explore the inland fog impact on aerosol chemistry
2 (Biswas et al., 2008; Safai et al., 2009). Fog, in fact, can be sampled only by specialist
3 fog samplers; however, during aerosol sampling at sea there is no way to avoid fog
4 once sea fog forms. Nevertheless, the effect of sea fog on aerosol chemistry has not
5 yet been well studied, not mentioning in the coastal and marginal seas of China where
6 air pollution is serious. Therefore, compared with inland fog and dust aerosols, we
7 have less knowledge about sea fog chemistry and the aerosol chemistry under sea fog
8 influence. This is the first investigation of Nr speciation and deposition of sea fog
9 modified aerosols (aerosol collected under sea fog influence) on the marginal seas off
10 a continent producing strong emissions.

11 Different types of aerosols may be composed of different amounts of nitrogen
12 species based on their formation history (e.g. origin, flow path, reactions during
13 transport). In this study, we sampled total suspended particulate (TSP) marine
14 aerosols on a cruise crossing over the ECSs and NWPO during spring 2014.
15 Water-soluble nitrogen species and ion characteristics among different aerosol types,
16 including dust, background and sea fog modified aerosols, were investigated. These
17 observational data promoted our understanding of the type-specific concentration and
18 deposition of various nitrogen species and the role of sea fog on nitrogen scavenging.
19 The data may aid in validating model outputs for the Asian region and potentially
20 evaluate the framework of nitrogen and aerosol interactions in current models.

21

22 **2 Materials and Methods**

23 **2.1 Aerosol sample collection and chemical analyses**

24 A total of 44 TSP samples were collected using a high-volume TSP aerosol sampler
25 (TE-5170D; Tisch Environmental Inc.) during a research cruise on the R/V
26 *Dongfanghong II* from 17 March to 22 April 2014. The cruise tracks (Fig. 1) covered
27 the ECSs and the NWPO. The samples were taken at ~ 12 h intervals. To avoid
28 self-contamination from the research vessel, we sampled only when the vessel was

1 cruising; thus, the sampling interval was not exactly 12 h. Based on simultaneous
2 one-second particle number concentration measurements made using an Optical
3 Particle Sizer (Tsi, US), we found that ship plumes affected the TSP sampling
4 occasionally during cruising (these data will be presented in a separate paper). We
5 calculated the plume contribution to the measured volume particle concentration of
6 PM₁₀ during each TSP sampling (self-contamination) and the short-period
7 contribution was less than 3%. Detailed sampling information including date, time
8 period and locations for each sample are listed in Table S1. Meteorological data (Fig.
9 2) including wind speed and direction, relative humidity (RH) and temperature were
10 recorded on-board.

11 The cruise encountered sea fog in the first few days (orange shadow in Fig. 2 for
12 17–19 March) and five samples (nos. 1–5) were collected. Surprisingly, sea fog
13 occurred again on 21–22 April while approaching land (samples nos. 43 and 44).
14 During the fog events, high RH and slow wind speed were recorded (see orange
15 shadow in Fig. 2). The strong temperature gradient indicated that the sea fog formed
16 owing to a cold air mass from land confronting warm air from the sea. Since these
17 samples were collected on fog days (see orange tracks in Fig. 1) when we could
18 collect aerosols, the sea fog modified the aerosols as well as sea fog droplets. Since
19 we could not separate them from each other through our method, we classified these
20 samples as “sea fog modified aerosol”.

21 Whatman 41 cellulose filters (Whatman Limited, Maidstone, UK) were used for
22 filtration. The analytical procedures were described by Hsu et al. (2010b and 2014).
23 Briefly, one-eighth of the filter was extracted using 15 mL of Milli-Q water on a
24 reciprocating shaker for 0.5 h and at rest for an additional 0.5 h at room temperature.
25 Then, the extract was filtered through a polycarbonate membrane filter (0.4 µm pore
26 size and 47 mm in diameter from Nuclepore). The filter was leached three times with
27 Milli-Q water, and then 5 mL Milli-Q water was used to rinse the filter. The extract 45
28 mL solution was mixed with the rinsing 5 mL, poured into a 50 mL clean plastic
29 centrifuge tube and used for the determination of the ion species and water-soluble

1 aluminum (Al).

2 The water soluble and total concentrations of Al in the TSPs were analyzed using
3 an inductively coupled plasma mass spectrometers (ICP-MS). For total Al, briefly,
4 one-eighth of the filter was digested with an acid mixture (4 mL HNO₃ + 2 mL HF)
5 using an ultra-high throughput microwave digestion system (MARSXpress, CEM;
6 Corporation, Matthews, NC), and the efficiency of the digestion scheme was checked
7 by subjecting a certain amount of a standard reference material (SRM1648, urban
8 particulate matter, National Institute of Standards and Technology, USA) to the same
9 treatment. The recoveries of Al in the SRM 1648 through digestion with the
10 HNO₃-HF mixture fell within $\pm 10\%$ ($n = 5$) of the certified values. Details regarding
11 the ICP-MS analysis were described by Hsu et al. (2008).

12 The major ionic species (Na⁺, NH₄⁺, K⁺, Mg²⁺, Ca²⁺, Cl⁻, NO₃⁻, NO₂⁻ and
13 SO₄²⁻) in the extract were analyzed using ion chromatography (model ICS-1100 for
14 anions and model ICS-900 for cations) equipped with a conductivity detector
15 (ASRS-ULTRA) and suppressor (ASRS-300 for the ICS-1100 and CSRS-300 for the
16 ICS-900). Separator columns (AS11-HC for anions, and CS12A for cations) and
17 guard columns (AG11-HC for anions and CG12A for cations) were used in the
18 analyses. The precision for all ionic species was better than 5%. Details of the
19 analytical processes can be found in Hsu et al. (2014). Only five samples contained
20 NO₂⁻ (1.39 nmol m⁻³ for no. 2, 2.32 nmol m⁻³ for no. 4, 3.69 nmol m⁻³ for no. 5, 5.96
21 nmol m⁻³ for no. 43 and 3.76 nmol m⁻³ for no. 44), which accounted for < 1% of the
22 total dissolved nitrogen (TDN).

23 The TDN was analyzed using the wet oxidation method to convert all nitrogen
24 species into nitrate with re-crystallized potassium persulfate, and then the
25 concentration of nitrate was measured using chemiluminescence (Knapp et al., 2005).
26 Monitoring with laboratory stock (NO₃⁻ + NH₄⁺ + Glycine + EDTA) showed that the
27 recoveries of TDN by the persulfate oxidizing reagent (POR) digestion fell within 95–
28 105% ($n = 6$) over the range of detection.

1 2.2 Data analysis

2 The amount of non-sea-salt Ca^{2+} (nss- Ca^{2+}) and non-sea-salt SO_4^{2-} (nss- SO_4^{2-}) in
3 the aerosol, and the Ca^{2+} and SO_4^{2-} fractions in excess over that expected from sea
4 salt, were calculated using the unit of equivalent concentration (neq m^{-3}) in the
5 following equations

6 $[\text{nss-}\text{Ca}^{2+}] = [\text{Ca}^{2+}] - [\text{ss-}\text{Ca}^{2+}]$, where $[\text{ss-}\text{Ca}^{2+}] = 0.044 \times [\text{Na}^+]$, (1)

7 $[\text{nss-}\text{SO}_4^{2-}] = [\text{SO}_4^{2-}] - [\text{ss-}\text{SO}_4^{2-}]$, where $[\text{ss-}\text{SO}_4^{2-}] = 0.121 \times [\text{Na}^+]$, (2)

8 where the factors 0.044 and 0.121 used above are the typical calcium-to-sodium and
9 sulfate-to-sodium equivalent molar ratios in seawater (Chester, 1990).

10 Relative acidity (RA) was calculated using all the observed ion species in their
11 equivalent concentrations following Yao and Zhang (2012):

12 $\text{RA} = ([\text{Na}^+] + [\text{Mg}^{2+}] + [\text{K}^+] + [\text{Ca}^{2+}] + [\text{NH}_4^+]) / ([\text{Cl}^-] + [\text{NO}_3^-] + [\text{SO}_4^{2-}])$, (3)

13 where $[\text{Na}^+]$, $[\text{Mg}^{2+}]$, $[\text{K}^+]$, $[\text{Ca}^{2+}]$, $[\text{NH}_4^+]$, $[\text{Cl}^-]$, $[\text{NO}_3^-]$ and $[\text{SO}_4^{2-}]$ are the
14 equivalent concentrations of those water extracted ions. The relative acidity is based
15 on the imbalance of cations and anions, which caused by the non-detected ions such
16 as H^+ , HCO_3^- and CO_3^{2-} (Kerminen et al., 2001). When the total ions were
17 distributed over a wide range (by a factor of 20 in our case), the ratio of total anions to
18 cations in neq m^{-3} is more effective in presenting the relative acidity than the absolute
19 value of imbalance (total cations – total anions).

20 The concentration of water-soluble organic nitrogen (WSON) was calculated using
21 the following equation:

22 $[\text{WSON}] = [\text{TDN}] - [\text{NO}_3^-] - [\text{NH}_4^+] - [\text{NO}_2^-]$, (4)

23 where $[\text{TDN}]$, $[\text{NO}_3^-]$, $[\text{NH}_4^+]$ and $[\text{NO}_2^-]$ are molar concentrations (nmol N m^{-3}) of
24 those water-soluble nitrogen species in TSPs. The standard errors propagated through
25 WSOn calculation varied from sample to sample (17 to 1500%). The average
26 standard error was 116% when all samples were considered and when the extreme
27 value was excluded the average standard error was reduced to 81%.

2.3 Flux calculation

The dry deposition flux (F) was calculated by multiplying the aerosol concentrations of water-soluble nitrogen speciation (C) by the dry deposition velocity (V):

$$4 \quad F = C \times V, \quad (5)$$

where V is a primarily function of particle size and meteorological parameters, such as wind speed, RH and sea surface roughness (Duce et al., 1991). According to previous reports, dry deposition velocity varies by more than 3 orders of magnitude at a particle size ranging from 0.1 to 100 μm (Hoppel et al., 2002). In general, ammonium appears in submicron mode from 0.1 to 1 μm with a small fraction residing in the coarser mode; on the contrary, nitrate is mainly distributed in a supermicron size ranging from 1 to 10 μm (Nakamura et al., 2005; Baker et al., 2010; Yao and Zhang, 2012; Hsu et al., 2014). The non-single-mode size distribution appears not just in nitrogenous elements but also metals including aluminum and iron (e.g., Baker et al., 2013). Thus, for any compound or elements by using a fixed deposition velocity to calculate dry deposition flux might cause under- or overestimation as discussed by Baker et al. (2013). Unfortunately, we collected TSPs with no information for size distributions. Not mentioning when the highly variable meteorological parameters were considered. In our observation wind speed ranging from 0.8 to 18 m s^{-1} under a RH ranging from 40 to 100% (Fig. 2). Thus, it is very difficult to provide variable dry deposition velocities under a wide range of environmental conditions (Hoppel et al., 2002; Baker et al., 2013); thus, assumptions were made based on existing knowledge. Based on the model and experimental results for aerosols deposition to the sea surface (Duce et al., 1991; Hoppel et al., 2002) and the size distribution of nitrate and ammonium in particles as reported above, deposition velocity of 2 cm s^{-1} was applied for nitrate and 0.1 cm s^{-1} for ammonium. Both deposition velocities were often used in calculating the specific nitrogen deposition fluxes, especially for the maritime aerosols, though uncertainties were involved (de Leeuw et al., 2003; Nakamura et al., 2005; Chen et al., 2010; Jung et al., 2013). As for WSON, the size distribution of WSON in previous studies showed that

1 WSON appears in a wide size spectrum (Chen et al., 2010; Lesworth et al., 2010;
2 Srinivas et al., 2011). In previous studies, different orders of magnitude of deposition
3 velocity were employed for WSON deposition (1.2 cm s^{-1} by He et al., 2011; 0.1 cm
4 s^{-1} for fine and 1.0 cm s^{-1} for coarse by Srinivas et al., 2011; 0.075 cm s^{-1} for fine and
5 1.25 cm s^{-1} for coarse by Violaki et al., 2010). Our TSP aerosols covered the entire
6 size distribution; thus, 1.0 cm s^{-1} was applied for WSON deposition. Since 1.0 cm s^{-1}
7 is near the upper boundary of velocities previously applied for WSON deposition, our
8 calculation of WSON deposition may represent the upper boundary.

9 Note that, a period of our aerosol sampling was influenced by sea fog, which we
10 could not avoid as mentioned earlier in the Introduction. Apparently, the deposition
11 velocity for sea fog modified aerosol differs from that of common aerosol, thus, the
12 deposition velocity needs to be revised once we have sufficient knowledge about the
13 influence of sea fog on aerosol deposition.

14 **2.4 Air mass backward trajectories analysis**

15 In order to investigate the likely origins of aerosols in the transporting air masses, 3
16 days with three heights of above sea level air mass backward trajectories were
17 calculated using the National Oceanic and Atmospheric Administration (NOAA)
18 Hybrid Single Particle Lagrangian Integrated Trajectory (HYSPLIT) model with a
19 $1^\circ \times 1^\circ$ latitude–longitude grid and the final meteorological database. Details about the
20 HYSPLIT model can be found at <https://ready.arl.noaa.gov/HYSPLIT.php>, as
21 prepared by the NOAA Air Resources Laboratory. The time period of 3 days was
22 suggested to be sufficient for dust transport from dust source to the NWPO (Husar et
23 al., 2001). The three heights (100, 500 and 1000 m) were selected because 1000 m
24 can be taken as one of the typical atmospheric boundary layers (Hennemuth and
25 Lammert, 2006).

26

27 **3 Results and discussion**

28 Using the Al content, air mass backward trajectories, weather conditions, and ion

1 stoichiometry, we classified aerosols into three types and then discussed the speciation
2 and concentrations of Nr for each aerosol type as well as the potential processes
3 involved. We compared the chemical characteristics of dust aerosols collected in the
4 ECSs with ours under sea fog influence. Global aerosol and precipitation WSON data
5 were also compiled to reveal the significance of WSON. Finally, we estimated the
6 deposition of individual nitrogen species for the three types of aerosol and highlighted
7 the importance of atmospheric nitrogen deposition in different regions.

8 **3.1 Aerosol type classification**

9 Total Al content in aerosol samples is an often used index to identify dust events (Hsu
10 et al., 2008). As shown in Fig. 3, the total Al concentrations in aerosols ranged from
11 52 to 6293 ng m⁻³ during our entire cruise. For the first three samples (from nos. 1 to 3
12 collected in the Yellow Sea), total Al increased from 1353 to 6293 ng m⁻³, and then
13 rapidly decreased (nos. 4 and 5 in the East China Sea) as the cruise moved eastward to
14 the NWPO (orange shadow in Fig. 3). When the cruise returned to the ECSs, the total
15 Al concentrations in the aerosols (nos. 43 and 44) increased once again. Apparently,
16 an abundance of dust is frequently present in the low atmosphere over the Chinese
17 marginal seas in spring. The air mass backward trajectories by HYSPLIT (Fig. 4a)
18 revealed that the air masses for these fog samples mainly hovered over the ECSs at an
19 altitude of < 500 m and the air masses for nos. 1–5 originated from the east coast of
20 China. The air masses for the samples of nos. 43–44 were from south of Korea. The
21 water-soluble Al followed the same pattern as total Al (Fig. 3) but the leachable
22 concentrations were significantly higher when compared with dust aerosols reported
23 for the same area. The relative acidity of aerosols showed that the values of sea fog
24 modified aerosols were all below 0.9 (Fig. 3) indicating an enhanced acidification
25 relative to those aerosols with sea fog influence. The low RA values explained the
26 higher concentrations of water-soluble Al.

27 As for sample nos. 6, 7, 25–27 and 29 collected in the NWPO (see pink tracks in
28 Fig. 1), the total Al concentrations ranged from 590 to 1480 ng m⁻³ with an average of

1 $1025 \pm 316 \text{ ng m}^{-3}$ (pink shadow in Fig. 3), which were significantly higher than the
2 remaining samples ($212 \pm 120 \text{ ng m}^{-3}$) from the NWPO. Although most of the air
3 mass backward trajectories of these samples collected in the NWPO originated from
4 25°N to 40°N (and beyond) as well as high altitude (Fig. 4b), the lidar browse images
5 from NASA (Fig. S1) clearly indicated that the air masses of these aerosol samples
6 pass through dusty regions. The consistency between high total Al concentration and
7 the occurrence of dust and polluted dust defined by the lidar browse images from the
8 NASA allowed us to separate dust aerosols from background aerosols. In this paper,
9 background aerosols stand for non-dusty and non-foggy aerosol in our classification.
10 It is more like a baseline aerosol collected within this study region during the
11 investigating period, thus, the “background” may vary over space and time and it does
12 not necessarily have to be pristine. Below we can also see a discernable ion
13 stoichiometry among the three types.

14 **3.2 Ion stoichiometry in three types of aerosol**

15 Excluding sea fog modified aerosols, all the ratios of total anions and total cations
16 followed close to a 1:1 linear relationship (Fig. 5a). Such a well-defined positive
17 relationship indicated the charge balance and further emphasized the validity of our
18 measurements. The sea fog modified aerosols in the ECSs contained higher contents
19 of anions than cations, which was consistent with previous observations for fog water
20 (Chang et al., 2002; Lange et al., 2003; Yue et al., 2014). The non-measured H^+ ion
21 should be the dominant cation for charge compensation as indicated previously
22 (Chang et al., 2002; Lange et al., 2003). The low RA values for sea fog modified
23 aerosols also supported this notion (Fig. 3). Below we set out the characteristics of the
24 three types of aerosol with ion stoichiometry.

25 Since the Cl^-/Na^+ ratios of all samples including sea fog modified aerosols (Fig.
26 5b) were near 1.17, this indicated that almost all the Na and Cl for our aerosols
27 originated from sea salt. The relationship between Mg^{2+} vs. Na^+ (Fig. 5c) indicated
28 that almost all Mg^{2+} also originated from sea salt sources ($\text{Mg}/\text{Na}_{ss} = 0.23$) except

1 sea fog modified aerosols, which held a deviated correlation due to Mg enrichment (y
2 = 0.32x + 8.7, R^2 = 0.88) because of terrestrial mineral sources of Mg. Such Mg
3 enrichment was not observed in summer sea fog in the subarctic North Pacific Ocean
4 (Jung et al., 2013).

5 As for Ca^{2+} (Fig. 5d), all types of aerosol were enriched in Ca^{2+} but at different
6 levels, indicating various degrees of terrestrial mineral influence on the marine
7 aerosols. For background aerosols, a strong correlation between Ca^{2+} and Na^+ ($y =$
8 $0.044x + 6.6$, R^2 = 0.92) was observed. The slope was identical to that of sea water
9 ($\text{Ca}/\text{Na}_{ss} = 0.044$) suggesting that most Ca^{2+} and Na^+ in background aerosols were
10 sourced from sea salt. An unusually high regression slope ($20 \times$ the sea salt) observed
11 between Ca^{2+} and Na^+ in sea fog modified aerosols ($y = 0.90x - 1.8$, R^2 = 0.71) was
12 attributable to the reaction between mineral CaCO_3 and H^+ in fog droplets during the
13 formation of sea fog (Yue et al., 2012). The more excessive Ca^{2+} observed in dust
14 aerosols implied that stronger heterogeneous reactions between the acid gas and dust
15 minerals had occurred during long-range transport (Hsu et al., 2014). Similar to Ca^{2+} ,
16 patterns between K^+ and Na^+ can also be seen in Fig. 5e. However, besides the
17 contribution from inland dust (Savoie and Prospero, 1980) excess K^+ may also
18 originate from biomass burning in China (Hsu et al., 2009). Note that statistically
19 significant intercepts could be seen in Ca^{2+} against Na_{ss} and K^+ against Na_{ss} scatter
20 plots for background aerosols. Although small, such excesses in Ca^{2+} and K^+
21 relative to Na^+ in widespread background aerosols warrant explanation.

22 As shown in Fig. 5f, a correlation was found between NH_4^+ and nss-SO_4^{2-} . Except
23 for three sea fog samples, all ratios fell close to the 1:1 regression line suggesting the
24 dominance of $(\text{NH}_4)_2\text{SO}_4$ rather than NH_4HSO_4 . Complete neutralization of NH_4^+ by
25 nss-SO_4^{2-} had likely occurred, and a similar phenomenon was found elsewhere (Zhang
26 et al., 2013; Hsu et al., 2014).

27 The ratio of $[\text{NO}_3^- + \text{nss-SO}_4^{2-}] / [\text{NH}_4^+ + \text{nss-Ca}^{2+}]$ for background aerosols (Fig.
28 5g) closely followed unity, thus suggesting that $\text{NH}_4^+ + \text{nss-Ca}^{2+}$ was neutralized by

the acidic ions NO_3^- and nss- SO_4^{2-} . However, for the dust and foggy aerosols, $[\text{NO}_3^- + \text{nss-SO}_4^{2-}] / [\text{NH}_4^+ + \text{nss-Ca}^{2+}]$ ratios located between 1:1 and 2:1 indicated that the excessive anthropogenic acidic ions that originated from coal fossil fuel combustion and vehicle exhaust had been transported to the ECSs and NWPO by the Asian winter monsoon as previously indicated (Hsu et al., 2010a). On the other hand, Liu et al. (2013) suggested that NHx emission in China is important and may play a major role in neutralizing the acidic ions. As shown in Fig. 5h, the scatter plot of NH_4^+ against NO_3^- , revealed that almost all dust and background aerosols sampled in the NWPO had $\text{NH}_4^+/\text{NO}_3^-$ ratios larger than 1, which is common in aerosol observation. However, significantly enriched NO_3^- in sea fog modified aerosols drew the ratio down to < 1 . Nevertheless, such relatively enriched nitrate to ammonium was consistent with a previous study of sea fog water collected from the South China Sea (Yue et al., 2012). In summary, the three types of aerosol had distinctive features in nitrogen speciation and ion stoichiometry including relative acidity (Fig. 6a) further supporting our aerosol type classification.

3.3 Nitrogen speciation and associated processes in different types of aerosol

3.3.1 Sea fog modified aerosols

Only a few studies concerning water-soluble nitrogen species in sea fog water were reported (Sasakawa and Uematsu, 2002; Yue et al., 2012; Jung et al., 2013). To the best of our knowledge, ours is the first first-hand data from the Chinese marginal seas (the ECSs) in spring concerning water-soluble nitrogen species in aerosols collected under the influence of sea fog. As shown in Table 1 and Fig. 6a, in sea fog modified aerosols the concentrations of nitrate ranged from 160 to 1118 nmol N m⁻³ with a mean of 536 ± 300 nmol N m⁻³ and ammonium was slightly lower than nitrate ranging from 228 to 777 nmol N m⁻³ with a mean of 442 ± 194 nmol N m⁻³. WSON in sea fog modified aerosols was the lowest nitrogen species ranging from 23 to 517

1 nmol N m⁻³ with a mean of 147 ± 171 nmol N m⁻³ (Table 1 and Fig. 6a). The sea fog
2 modified aerosols contained 2–11 times higher concentration of nitrate, 2–6 times
3 higher ammonium and 3–6 times higher WSON when compared with aerosols in the
4 ECSs and other regions (Table 1). Such high concentrations of Nr not only
5 highlighted the seriousness of the nitrogen air pollution in Chinese marginal seas, but
6 also underscored that water-soluble nitrogen species can be scavenged efficiently
7 during sea fog formation.

8 Since none chemistry data of sea fog modified aerosols had been reported before,
9 we can only compare with the dust aerosols from the same regions in spring. The
10 concentrations of leachable ions, water-soluble and total Al and RA for dust aerosols
11 and sea fog modified aerosols sampled in the ECSs were listed in Table 2. The seven
12 sea fog modified aerosols were distinctive in chemical characteristics. For all except
13 NH₄⁺, NO₃⁻ and SO₄²⁻, sea fog modified aerosols had lower or similar molar
14 concentrations relative to dust aerosols. The anthropogenic species, particularly NO₃⁻
15 and NH₄⁺, were the most abundant ions in the sea fog modified aerosols. On the
16 contrary, Na⁺ and Cl⁻ were the highest among all the ions in dust aerosols from the
17 island of Jeju and the East China Sea. Taking Jeju as an example, the concentration
18 levels of Na⁺ and Cl⁻ were similar to those of our sea fog modified aerosols, yet
19 both NO₃⁻ and NH₄⁺ in sea fog modified aerosols were > 6 times higher than those
20 from the island of Jeju.

21 The pie charts for ion fractions of aerosols from the ECSs were shown in Fig. 7.
22 Note that the fraction distribution of ions for the dust aerosols from a previous cruise
23 in the ECS (n = 8, Fig. 7b, Hsu et al., 2010b) resembled that collected from the island
24 of Jeju (n = 49, Fig. 7c, Kang et al., 2009) despite the fact that their sampling were in
25 different spaces and at different times. Such consistency in the ion pie chart indicated
26 the representativeness of these dust aerosols. However, the pie chart for sea fog
27 modified aerosols revealed that NH₄⁺ and NO₃⁻ occupied approximately 30 and 36%
28 of the total ionic concentration (Fig. 7a). Such an overwhelmingly high occupation of
29 nitrogenous ions emphasized the role of sea fog in modifying the chemistry of

1 non-foggy dust aerosols.

2 In a previous study in the Po Valley, the average scavenging efficiency for aerosol
3 nitrate and ammonium were reported to be at similar levels (70 and 68%; Gilardoni et
4 al., 2014), while in our case the concentrations of nitrate in sea fog modified aerosols
5 were higher than those of ammonium (Table 1 and Fig. 6a). Since the gas phase
6 HNO_3 is rapidly dissolved in liquid water particles during the early stages of fog
7 formation (Fahey et al., 2005; Moore et al., 2004), it was reasonable to infer that the
8 enriched nitrate in sea fog was attributed to gaseous HNO_3 owing to the gas–liquid
9 equilibrium between NO_3^- and HNO_3 in fog droplets. Moreover, our sea fog
10 modified aerosols were collected from the air masses roaming around east China and
11 the ECSs, where the NO_x emission is the highest in China (Gu et al., 2012). The
12 lifetime of NO_x in the boundary layer is generally less than 2 days (Liang et al., 1998).
13 Based on our air mass backward trajectories analysis, the travel time of air masses
14 from inland China to the marginal seas is long enough for oxidation of NO_x into
15 HNO_3 . Thus, nitrate enrichment in the sea fog modified aerosol was likely a
16 synergistic consequence due to the sea fog formation and gas–liquid equilibrium of
17 gaseous HNO_3 .

18 As for SO_4^{2-} , both the concentration and percentage occupation were comparable
19 in sea fog modified aerosols and dust aerosols (Table 2 and Fig. 7). However, the
20 concentrations of nss- SO_4^{2-} in sea fog modified aerosols was 60% higher than those
21 of dust aerosols (Table 2), suggesting the addition of anthropogenic SO_x emission
22 during sea fog formation as indicated by Gilardoni et al. (2014). In the marginal seas
23 adjacent to the anthropogenic emission source, acidified sea fog induced by additional
24 sulfuric and nitric acid was common (Sasakawa and Uematsu, 2005; Yue et al., 2014).
25 In general, Al in marine aerosols originated from terrestrial minerals (Uematsu et al.,
26 2010). The mean concentrations of total Al in our seven sea fog samples were the
27 lowest among those in dust aerosols from the ECSs (Table 2). However, the
28 concentrations as well as the fractions of water-soluble Al in sea fog modified
29 aerosols were significantly higher than those of dust aerosols. Because of the high

1 acidity (low RA values) for sea fog modified aerosols (Fig. 6a), we suspected that
2 during the seasonal transition period the formation of sea fog at the land–ocean
3 boundary may acidify the aerosol to effectively promote the solubility of metals in
4 aerosol minerals.

5 Finally, it has been shown that dissolved organic matter can be scavenged by fog,
6 but its scavenging efficiency was lower than those of nitrate and ammonium due to
7 hydrophobic organic species were more difficult to be scavenged than hydrophilic
8 ones (Maria and Russell, 2005; Gilardoni et al., 2014). In our case, although
9 concentrations of WSON in sea fog modified aerosols ($147 \pm 171 \text{ nmol N m}^{-3}$) were
10 significantly higher than those of background aerosols, the ratio of WSON to TDN in
11 sea fog modified aerosols ($10 \pm 6\%$) was similar to those (ranging from 10 to 24%) of
12 background aerosols sampled in the ECSs (Table 1). Such high WSON concentration
13 but low WSON% in TDN in sea fog modified aerosols may indicate the lower
14 scavenging efficiency of WSON relative to other nitrogen species or that its source
15 region is different or both.

16 Note that all these aerosols in our study were sampled by TSP. Conventional
17 knowledge indicates that aerosol may act as a precursor for fog formation, but this
18 does not necessarily mean all the aerosols we sampled were directly associated with
19 fog. Nevertheless, we observed distinctive chemistry for this type of aerosol either
20 comparing with aerosols sampled during the same cruise or comparing with
21 “non-foggy” aerosols collected in the ECS in previous study. More studies are needed
22 to explore the effect of sea fog formation on aerosol chemistry.

23 3.3.2 Dust aerosols

24 For dust aerosols collected in the NWPO, nitrate ranged from 79 to $145 \text{ nmol N m}^{-3}$
25 with an average of $100 \pm 23 \text{ nmol N m}^{-3}$, and ammonium ranged from 94 to 163 nmol
26 N m^{-3} with an average of $138 \pm 24 \text{ nmol N m}^{-3}$ (Table 1 and Fig. 6a). Relative to
27 background aerosols, both nitrate and ammonium were significantly higher in dust
28 aerosols revealing the anthropogenic nitrogen fingerprint carried by the Asian dust

1 outflow along with westerlies (Chen and Chen, 2008). Interestingly, dust aerosols
2 contained a low concentration of WSON ($11.2 \pm 4.0 \text{ nmol N m}^{-3}$) resembling that of
3 background aerosols (Table 1 and Fig. 6a). Moreover, dust aerosols held the lowest
4 WSON fraction in total dissolved nitrogen among the three types (Table 1 and Fig.
5 6b). Based on the good correlation between nss-Ca²⁺ and WSON, previous studies
6 demonstrated that dust can carry anthropogenic “nitrogen” activity into remote oceans
7 and simultaneously promote the ratio of WSON /TDN in aerosol (Mace et al., 2003b;
8 Lesworth et al., 2010; Violaki et al., 2010). However, in our case there was no
9 correlation between WSON and nss-Ca²⁺ (not shown), likely illustrating that these
10 aerosols had less chance to contact WSON along their pathway from a high altitude,
11 or that WSON had been scavenged during transport. However, the latter was less
12 likely.

13 3.3.3 Background aerosols

14 For the 31 background aerosol samples, the mean concentrations of NO₃⁻ and NH₄⁺
15 were 26 ± 32 and $54 \pm 45 \text{ nmol N m}^{-3}$ (Table 1). Both were 10 times higher than those
16 collected in the same region during summer ($2.5 \pm 1.0 \text{ nmol N m}^{-3}$ for nitrate and $5.9 \pm 2.9 \text{ nmol N m}^{-3}$ for ammonium; Jung et al., 2011). The 10 times higher Nr for
17 springtime background aerosols indicated that the “spring background” was not
18 pristine at all. Such distinctive seasonality was ascribed to the origins of air mass,
19 since in summer the air masses in our study area were mainly from the open ocean
20 while in spring the air masses came from the northeast of China through the Japanese
21 Sea and Japan (Fig. 4c), where they were strongly influenced by anthropogenic
22 nitrogen emission (Kang et al., 2010). The concentration of WSON in background
23 aerosols was $10.9 \pm 6.8 \text{ nmol N m}^{-3}$, which fell within the wide range reported
24 previously (~1 to 76 nmol N m^{-3} ; Table 1). In the open ocean, the WSON in aerosols
25 may come from natural and anthropogenic sources. For example, the highest
26 percentage of WSON in TDN in the southern Atlantic (84%) was attributed to high
27 biological productivity (Violaki et al., 2015). Unfortunately, no marine biological data

1 (i.e. special amines or amino acids as summarized by Cape et al., 2011) existed in our
2 case to directly support marine sourced aerosol WSON.

3 Nevertheless, our sampling cruise experienced a wide range of wind speed with
4 variable sea salt contents during the collection of background aerosols. The
5 correlations between ion content and wind speed may reveal some useful information
6 as indirect evidence. Higher sea salt, e.g. Na^+ , Cl^- , Mg^{2+} , appeared with higher
7 wind speed conditions (Fig. 8a-c). Positive correlations can be seen although r square
8 values were small possibly due to time-integrated sampling (~12 h) and averaged
9 wind speed over the sampling period. The positive correlation illustrated that the
10 emission of sea salt aerosols was driven by wind intensity as indicated by Shi et al.
11 (2012). Except for WSON (Fig. 8d), which was consistent with sea salt associated
12 ions, no statistically significant relationships can be derived from scatter plots of
13 nitrate and ammonium against wind speed (Fig. 8e and f). An analogous tendency
14 between WSON and sea salt ions suggested that WSON might come from the surface
15 ocean. Since the concentration of dissolved organic nitrogen (DON) in surface sea
16 water was less variable, ranging from 4.5 to 5.0 μM in the Pacific Ocean (Knapp et al.,
17 2011), DON can be taken as a relatively constant component in surface sea water
18 similar to Na^+ , Cl^- and Mg^{2+} . Very likely, breaking waves and sea spray brought
19 DON into the atmosphere under higher wind speed. In fact, using free amino acids
20 and urea compositions in the maritime aerosol, Mace et al. (2003a) indicated that live
21 species in the sea surface microlayer may serve as a source of atmospheric organic
22 nitrogen.

23 Compared with DON in the surface ocean, it is not possible that nitrate and
24 ammonium in the surface seawater are a source of atmospheric aerosol nitrate and
25 ammonium since the concentrations of nitrate and ammonium are very low (a few
26 tens to hundreds of nM) in the surface ocean. However, under a wide range of wind
27 speed, we observed relatively narrow concentration ranges of aerosol ammonium and
28 nitrate. This was strange, given that high wind speed implied vigorous exchange on
29 the air-sea interface, during which both sea salt emission and scavenging were

1 supposed to be high. Under efficient scavenging conditions, to maintain a relatively
2 uniform aerosol nitrate or ammonium concentration (quasi-static), some supply
3 processes are needed for compensation. Since the surface ocean is not a possible
4 source for both aerosol ammonium and nitrate, we suggested alternative supplies
5 which included deposition from the upper atmosphere and photochemical
6 production/consumption.

7 Based on $\delta^{15}\text{N}-\text{NH}_4^+$ in aerosol (Jickells et al., 2003) and rainwater (Altieri et al.,
8 2014) collected in the Atlantic, the ocean was suggested to be one of the ammonium
9 sources for the atmosphere. Because of the low concentration of ammonium in the
10 ocean surface, direct ammonium emission via sea spray was less likely. Based on our
11 observation, we hypothesized that the emitted marine WSON in the atmosphere may
12 serve as a precursor for ammonium and/or nitrate via the photo-degradation and
13 photo-oxidation processes reported previously (Spokes and Liss, 1996; Vione et al.,
14 2005; Xie et al., 2012). A most recent study by Paulot et al. (2015) supported our
15 hypothesis. By modeling global inventories of ammonia emissions, they found that
16 the ammonia source from the ocean cannot neutralize the sulfate aerosol acidity, thus
17 photolysis of marine DON at the ocean surface or in the atmosphere was suggested to
18 be a source of atmospheric ammonia. More studies about the exchange processes
19 among nitrogen species through the ocean–atmosphere boundary layer are needed.

20 **3.4 WSON in aerosol and rainwater: a global comparison**

21 Organic nitrogen, distributed in the gas, particulate and dissolved phases, is an
22 important component in the atmospheric nitrogen cycle. In our case, mean fractions of
23 WSON in aerosol TDN were 10 ± 6 , 5 ± 2 and $14 \pm 8\%$ for modified sea fog, dust and
24 background aerosols. All values fell within the wide range reported previously (also in
25 Table 1). Here we synthesized a published data set about aerosol WSON from around
26 the world for comparison (Fig. 9a). The synthesized data revealed that aerosol WSON
27 concentrations varied over 3 orders of magnitude and the fraction of WSON in TDN
28 ranged from 1% to as high as 85%. Additionally, the fraction of WSON was the less

1 variable towards high WSON concentrations. The slope of the linear regression
2 between WSON and TDN indicated that WSON accounted for 18% of aerosol TDN.
3 Although the positive correlation between WSON and TDN may imply WSON's
4 anthropogenic origin (Jickells et al., 2013), the marine sourced WSON cannot be
5 ignored in the open ocean as discussed in Section 3.3.3.

6 In Fig. 9b, we made a comparison between the distribution of the WSON fraction
7 in rainwater TDN and that in aerosol. The distribution pattern of WSON fractions in
8 aerosols (Fig. 9b, grey bar) was relatively concentrated revealing a tendency towards
9 lower fractions. Its peak frequency appeared at the category of 10–20% and at least 80%
10 of the observed WSON fractions fell within the range < 25%. However, for
11 WSON/TDN in rainwater (Fig. 9b, blue bar), the distribution pattern was relatively
12 diffusive shifting towards a higher percentage and peaking at around categories of 25–
13 40% with a mean value of 33% ($n = 332$), which is slightly higher than that (24%, $n =$
14 115) obtained by Jickells et al. (2013). Although values of the coefficient of variation
15 for both aerosol and rainwater were high, the results were still statistically meaningful.
16 The mean WSON fraction for rainwater was around 2 times that for aerosol (18%),
17 but the sampling bias inherited in such comparison should be noted. In a previous
18 study, Mace et al. (2003a) reported that the fractional contribution of dissolved free
19 amino acids to organic nitrogen in rainwater was 4 times higher than that in aerosol.
20 The higher fractional contribution of WSON to TDN for rainwater may imply that
21 precipitation washed out hydrophilic organic matter or WSON from the atmosphere
22 more effectively (Maria and Russell, 2005).

23 **3.5 Dry deposition of TDN and the implications**

24 As shown in Fig. 10, the atmospheric nitrogen dry deposition over the cruise revealed
25 a large spatial variance under different weather conditions. In the ECSs, the mean
26 DIN ($\text{NH}_4^+ + \text{NO}_3^-$) deposition on fog days was estimated to be $\sim 960 \mu\text{mol N m}^{-2} \text{d}^{-1}$
27 (926 ± 518 and $38 \pm 17 \mu\text{mol N m}^{-2} \text{d}^{-1}$ for nitrate and ammonium), which was around
28 6 times higher than the average values for ordinary aerosols derived from literature

1 reports ($153 \mu\text{mol N m}^{-2} \text{d}^{-1}$ for aerosol nitrate and $12.3 \mu\text{mol N m}^{-2} \text{d}^{-1}$ for aerosol
2 ammonium; see Table 3). The WSON deposition ranged from 20 to $446 \mu\text{mol N m}^{-2} \text{d}^{-1}$
3 with an average of $127 \pm 148 \mu\text{mol N m}^{-2} \text{d}^{-1}$. Since the bioavailability of aerosol
4 WSON to phytoplankton was reported to be high (12–80%; Bronk et al., 2007;
5 Wedyan et al., 2007), by adding WSON into consideration, the deposition of TDN
6 will be $\sim 1100 \mu\text{mol N m}^{-2} \text{d}^{-1}$.

7 Taking $1150 \times 10^3 \text{ km}^2$ for the total area cover by the ECSs, we calculated the daily
8 nitrogen supply from atmospheric deposition associated with sea fog to be $18 \pm 11 \text{ Gg}$
9 TDN d^{-1} , which is around 6 times the nitrogen input from the Yangtze River in spring
10 (total amount of $3.1 \text{ Gg DIN d}^{-1}$; Li et al., 2011) and 2 times the supply from the
11 subsurface intrusion of the Kuroshio ($7.9 \text{ Gg NO}_3^- \text{-N d}^{-1}$; Chen, 1996). In the ECSs,
12 the sea fog occurrence was around 3–5 days in March and 8–10 days in April (Zhang
13 et al., 2009). Given such high TDN deposition per day, the contribution of foggy
14 weather should really be taken into account on a monthly estimate even though the
15 occurrence of sea fog is limited in time and space. Moreover, the atmospheric
16 influence is more widespread than the river focusing on the plume area.

17 Assuming that nitrogen was the limiting nutrient and that all the total dissolved
18 nitrogen deposited from atmosphere into the sea was bioavailable and would be
19 utilized for carbon fixation, we obtained a C-fixation rate of $\sim 87 \text{ mg C m}^{-2} \text{d}^{-1}$ in
20 spring for the ECSs based on the Redfield C/N ratio of 6.6. Since atmospheric
21 nitrogen deposition is an external source, such a conversion represents new
22 production. When compared with the primary productivity in the East China Sea
23 ($292\text{--}549 \text{ mg C m}^{-2} \text{d}^{-1}$; Gong et al., 2000), the new production associated with sea
24 fog nitrogen deposition may account for 16–30% of the primary production in the
25 ECSs on foggy days in spring.

26 Similar to sea fog on the ECSs, sporadic dust events are frequently observed from
27 March to May in the NWPO (Shao and Dong, 2006). In our spring case, the average
28 deposition of dust aerosol nitrate and ammonium ($172 \pm 40 \mu\text{mol N m}^{-2} \text{d}^{-1}$ for nitrate
29 and $11.9 \pm 2.1 \mu\text{mol N m}^{-2} \text{d}^{-1}$ for ammonium) were significantly higher than that of

1 background aerosols ($44.6 \pm 55.3 \mu\text{mol N m}^{-2} \text{ d}^{-1}$ for nitrate and $4.7 \pm 4.0 \mu\text{mol N m}^{-2} \text{ d}^{-1}$ for ammonium; see Table 3). However, both dust and background aerosols depositions were significantly higher in spring when compared to summer dry deposition in the subtropical western North Pacific ($3.0 \pm 1.5 \mu\text{mol N m}^{-2} \text{ d}^{-1}$ for nitrate and $2.7 \pm 2.1 \mu\text{mol N m}^{-2} \text{ d}^{-1}$ for ammonium) and the subarctic western North Pacific ($3.3 \pm 2.3 \mu\text{mol N m}^{-2} \text{ d}^{-1}$ for nitrate and $1.9 \pm 0.63 \mu\text{mol N m}^{-2} \text{ d}^{-1}$ for ammonium) (Jung et al., 2011). Likewise, the C-fixation rate in the NWPO during spring was estimated to be $4.5\text{--}15 \text{ mg C m}^{-2} \text{ d}^{-1}$ based on the above assumptions and observations. The minimal level of C-fixation induced by dry deposition, in fact, equals to the maximum carbon uptake ($3.6 \text{ mg C m}^{-2} \text{ d}^{-1}$; Jung et al., 2013) in summer by the total atmospheric DIN deposition (wet + dry + sea fog) in the western North Pacific Ocean. Thus, the contribution of atmospheric nitrogen deposition to primary production in the NWPO could be significantly different between seasons.

14

15 4 Conclusions

16 We presented the total dissolved nitrogen species including water-soluble organic
17 nitrogen in TSP sampled over the ECSs and NWPO during spring and the samples of
18 the ECSs were collected under sea fog influence. Three types of aerosol, the sea fog
19 modified, the dust and the background aerosols, were classified. We found that sea
20 fog formation significantly altered the aerosol chemistry resulting in the highest
21 concentrations of all nitrogen species among the three types of aerosol, accompanied
22 with higher acidity and higher cation deficiency. On a daily basis, the nitrogen supply
23 from sea fog associated atmospheric deposition into the ECSs was around 6 times the
24 nitrogen supply from the Yangtze River in spring (total amount of $3.1 \text{ Gg DIN d}^{-1}$)
25 and 2 times the supply from the subsurface intrusion of Kuroshio ($7.9 \text{ Gg NO}_3^- \text{-N d}^{-1}$).
26 Sea fog associated deposition and chemical processes require more attention and need
27 to be considered in future aerosol monitoring and modeling works especially in
28 marginal seas during seasonal transition.

29 In the open sea, the spring background aerosol ammonium and nitrate were 10

1 times higher than previous report for summer indicating an anthropogenic influence
2 and the importance of the seasonality of the air mass source. The ammonium and
3 nitrate varied in narrow ranges showing no correlation with wind speed, which may
4 represent the degree of sea salt emission and scavenging. It is likely that nitrate and
5 ammonium in the atmosphere above sea surface had reached a budget balance. Since
6 the supply of nitrate and ammonium from surface ocean (bottom) is not possible, their
7 sources might come from upper atmospheric boundary layer (top) or photochemical
8 production of nitrogenous compounds. On the contrary, WSON revealed a similar
9 pattern to the sea salt ions (Na^+ , Mg^{2+} and Cl^-), in which concentrations increased
10 as the wind speed increased. Such a similarity indicated that at least a portion of the
11 WSON should come from the surface ocean where DON emitted with sea salt. Future
12 studies of nitrogen isotopic compositions of aerosol WSON and marine DON may
13 shed light on the role of marine DON in nitrogen cycling of the air-sea interface.

14 The dust aerosols were significantly enriched in nitrate and ammonium, but not in
15 WSON. Unless WSON-depletion processes had occurred, such a disproportionate
16 enrichment suggested that dust aerosols from high latitude and altitude may have less
17 chance to contact WSON during long range transport.

18 The WSON to TDN ratios of aerosols collected in the ECSs and NWPO fell within
19 that of the global pattern of aerosols. Since nitrate and ammonium are mainly
20 anthropogenic, the significantly positive correlation between WSON and TDN may
21 imply WSON's anthropogenic origin. When TDN concentrations were low (<100
22 nmol m^{-3}), the proportions of WSON in TDN were more diffusive indicating that
23 factors other than anthropogenic ones were involved. The mean ratio of WSON to
24 TDN in aerosols was only 1/2 of that for precipitation over the world. Such a low
25 proportion of WSON in aerosol TDN suggested that the aerosol was less capable of
26 scavenging hydrophilic organic nitrogen when compared with precipitation.
27 Nevertheless, WSON occupies a significant portion of the TDN for both aerosol and
28 precipitation and, thus, cannot be overlooked in the atmospheric nitrogen cycle.

29

1 **Acknowledgements**

2 This research was funded by the Major State Basic Research Development Program
3 of China (973 program) (nos. 2014CB953702 and 2015CB954003), and the National
4 Natural Science Foundation of China (NSFC U1305233, 91328207 and 41121091).
5 We also thank Peirang Yu and Tianfeng Guo (Ocean University of China) for helping
6 us to collect samples during the cruise and Shuen-Hsin Lin (Academia Sinica in
7 Taiwan) for help in chemical analyses. Professor John Hodgkiss of The University of
8 Hong Kong is thanked for his assistance with English.

9

10 **References**

- 11 Altieri, K. E., Hastings, M. G., Peters, A. J., and Sigman, D. M.: Molecular
12 characterization of water soluble organic nitrogen in marine rainwater by ultra-high
13 resolution electrospray ionization mass spectrometry, *Atmos. Chem. and Phys.*, 12,
14 3557–3571, doi:10.5194/acp-12-3557-2012, 2012.
- 15 Altieri, K., Hastings, M., Peters, A., Oleynik, S., and Sigman, D.: Isotopic evidence
16 for a marine ammonium source in rainwater at Bermuda, *Global Biogeochem. Cy.*,
17 28, 1066–1080, 2014.
- 18 Baker, A., Lesworth, T., Adams, C., Jickells, T., and Ganzeveld, L.: Estimation of
19 atmospheric nutrient inputs to the Atlantic Ocean from 50°N to 50°S based on
20 large-scale field sampling: Fixed nitrogen and dry deposition of phosphorus, *Global
21 Biogeochem. Cy.*, 24, GB3006, doi: 10.1029/2009GB003634, 2010.
- 22 Baker, A., Adams, C., Bell, T., Jickells, T., and Ganzeveld, L.: Estimation of
23 atmospheric nutrient inputs to the Atlantic Ocean from 50°N to 50°S based on
24 large-scale field sampling: Iron and other dust-associated elements, *Global
25 Biogeochem. Cy.*, 27, 755–767, 2013.
- 26 Biswas, K., Ghauri, B., and Husain, L.: Gaseous and aerosol pollutants during fog and
27 clear episodes in South Asian urban atmosphere, *Atmos. Environ.*, 42, 7775–7785,
28 2008.

- 1 Bronk, D. A., See, J. H., Bradley, P., and Killberg, L.: DON as a source of
2 bioavailable nitrogen for phytoplankton, *Biogeosciences*, 4, 283–296,
3 doi:10.5194/bg-4-283-2007, 2007.
- 4 Cape, J. N., Cornell, S. E., Jickells, T. D., and Nemitz, E.: Organic nitrogen in the
5 atmosphere-Where does it come from? A review of sources and methods, *Atmos.*
6 *Res.*, 102, 30–48, 2011.
- 7 Chang, S.-C., Lai, I.-L., and Wu, J.-T.: Estimation of fog deposition on epiphytic
8 bryophytes in a subtropical montane forest ecosystem in northeastern Taiwan,
9 *Atmos. Res.*, 64, 159–167, 2002.
- 10 Chen, C.: The Kuroshio intermediate water is the major source of nutrients on the
11 East China Sea continental shelf, *Oceanol. Acta*, 19, 523–527, 1996.
- 12 Chen, H.-Y. and Chen, L.-D.: Importance of anthropogenic inputs and
13 continental-derived dust for the distribution and flux of water-soluble nitrogen and
14 phosphorus species in aerosol within the atmosphere over the East China Sea, *J.*
15 *Geophys. Res.*, 113, D11303, doi:10.1029/2007jd009491, 2008.
- 16 Chen, H. Y., Chen, L. D., Chiang, Z. Y., Hung, C. C., Lin, F. J., Chou, W. C., Gong, G.
17 C., and Wen, L. S.: Size fractionation and molecular composition of water-soluble
18 inorganic and organic nitrogen in aerosols of a coastal environment, *J. Geophys.*
19 *Res.-Atmos.*, 115, D22307, doi:10.1029/2010JD014157, 2010.
- 20 Chen, Y., Mills, S., Street, J., Golan, D., Post, A., Jacobson, M., and Paytan, A.:
21 Estimates of atmospheric dry deposition and associated input of nutrients to Gulf of
22 Aqaba seawater, *J. Geophys. Res.-Atmos.*, 112, D04309, doi:10.1029/2006JD
23 007858, 2007.
- 24 Chen, Y.-X., Chen, H.-Y., Wang, W., Yeh, J.-X., Chou, W.-C., Gong, G.-C., Tsai, F.-J.,
25 Huang, S.-J., and Lin, C.-T.: Dissolved organic nitrogen in wet deposition in a
26 coastal city (Keelung) of the southern East China Sea: origin, molecular
27 composition and flux, *Atmos. Environ.*, 112, 20–31, 2015.

- 1 Chester, R.: Marine Geochemistry. Cambridge Univ. Press, London, 1990.
- 2 Cornell, S. E.: Atmospheric nitrogen deposition: revisiting the question of the
3 importance of the organic component, Environ. Pollut., 159, 2214–2222, 2011.
- 4 Cui, J., Zhou, J., Peng, Y., He, Y. Q., Yang, H., Xu, L. J., and Chan, A.: Long-term
5 atmospheric wet deposition of dissolved organic nitrogen in a typical red-soil
6 agro-ecosystem, Southeastern China, Environ. Sci. Processes Impacts, 16, 1050–
7 1058, 2014.
- 8 de Leeuw, G., Spokes, L., Jickells, T., Skjøth, C. A., Hertel, O., Vignati, E., Tamm, S.,
9 Schulz, M., Sørensen, L.-L., and Pedersen, B.: Atmospheric nitrogen inputs into the
10 North Sea: effect on productivity, Cont. Shelf Res., 23, 1743–1755, 2003.
- 11 Duce, R., Unni, C., Ray, B., Prospero, J., and Merrill, J.: Long-range atmospheric
12 transport of soil dust from Asia to the tropical North Pacific: temporal variability,
13 Science, 209, 1522–1524, 1980.
- 14 Duce, R., Liss, P., Merrill, J., Atlas, E., Buat-Menard, P., Hicks, B., Miller, J.,
15 Prospero, J., Arimoto, R., and Church, T.: The atmospheric input of trace species to
16 the world ocean, Global Biogeochem. Cy., 5, 193–259, 1991.
- 17 Duce, R., LaRoche, J., Altieri, K., Arrigo, K., Baker, A., Capone, D., Cornell, S.,
18 Dentener, F., Galloway, J., and Ganeshram, R.: Impacts of atmospheric
19 anthropogenic nitrogen on the open ocean, Science, 320, 893–897, 2008.
- 20 Fahey, K., Pandis, S., Collett, J., and Herckes, P.: The influence of size-dependent
21 droplet composition on pollutant processing by fogs, Atmos. Environ., 39, 4561–
22 4574, 2005.
- 23 Galloway, J. N., Townsend, A. R., Erisman, J. W., Bekunda, M., Cai, Z., Freney, J. R.,
24 Martinelli, L. A., Seitzinger, S. P., and Sutton, M. A.: Transformation of the
25 nitrogen cycle: recent trends, questions, and potential solutions, Science, 320, 889–
26 892, 2008.
- 27 Gilardoni, S., Massoli, P., Giulianelli, L., Rinaldi, M., Paglione, M., Pollini, F.,

- 1 Lanconelli, C., Poluzzi, V., Carbone, S., and Hillamo, R.: Fog scavenging of
2 organic and inorganic aerosol in the Po Valley, *Atmos. Chem. Phys.*, 14, 6967–6981,
3 doi:10.5194/acp-14-6967-2014, 2014.
- 4 Gong, G.-C., Shiah, F.-K., Liu, K.-K., Wen, Y.-H., and Liang, M.-H.: Spatial and
5 temporal variation of chlorophyll a, primary productivity and chemical
6 hydrography in the southern East China Sea, *Cont. Shelf Res.*, 20, 411–436, 2000.
- 7 Gu, B., Ge, Y., Ren, Y., Xu, B., Luo, W., Jiang, H., Gu, B., and Chang, J.:
8 Atmospheric reactive nitrogen in China: sources, recent trends, and damage costs,
9 *Environ. Sci. Technol.*, 46, 9420–9427, 2012.
- 10 Guenther, A., Karl, T., Harley, P., Wiedinmyer, C., Palmer, P. I., and Geron, C.:
11 Estimates of global terrestrial isoprene emissions using MEGAN (Model of
12 Emissions of Gases and Aerosols from Nature), *Atmos. Chem. Phys.*, 6, 3181–3210,
13 doi:10.5194/acp-6-3181-2006, 2006.
- 14 He, J., Balasubramanian, R., Burger, D. F., Hicks, K., Kuylestierna, J. C., and Palani,
15 S.: Dry and wet atmospheric deposition of nitrogen and phosphorus in Singapore,
16 *Atmos. Environ.*, 45, 2760–2768, 2011.
- 17 Hennemuth, B., and Lammert, A.: Determination of the atmospheric boundary layer
18 height from radiosonde and lidar backscatter, *Bound.-Lay. Meteorol.*, 120, 181–200,
19 2006.
- 20 Hoppel, W., Frick, G., and Fitzgerald, J.: Surface source function for sea-salt aerosol
21 and aerosol dry deposition to the ocean surface, *J. Geophys. Res.-Atmos.*, 107,
22 AAC 7-1–AAC 7-17, doi:10.1029/2001JD002014, 2002.
- 23 Hsu, S. C., Liu, S. C., Huang, Y. T., Lung, S. C. C., Tsai, F., Tu, J. Y., and Kao, S. J.: A
24 criterion for identifying Asian dust events based on Al concentration data collected
25 from northern Taiwan between 2002 and early 2007, *J. Geophys. Res.-Atmos.*, 113,
26 D18306, doi:10.1029/2007JD009574, 2008.
- 27 Hsu, S.-C., Liu, S. C., Huang, Y.-T., Chou, C. C. K., Lung, S. C. C., Liu, T.-H., Tu,

- 1 J.-Y., and Tsai, F.: Long-range southeastward transport of Asian biosmoke pollution:
2 signature detected by aerosol potassium in Northern Taiwan, *J. Geophys. Res.*, 114,
3 D18306, doi:10.1029/2007JD009574, doi:10.1029/2009jd011725, 2009.
- 4 Hsu, S., Liu, S., Tsai, F., Engling, G., Lin, I., Chou, C., Kao, S., Lung, S., Chan, C.,
5 and Lin, S.: High wintertime particulate matter pollution over an off shore island
6 (Kinmen) off southeastern China: an overview, *J. Geophys. Res.-Atmos.*, 115,
7 D17309, doi:10.1029/2009JD013641, 2010a.
- 8 Hsu, S.-C., Wong, G. T. F., Gong, G.-C., Shiah, F.-K., Huang, Y.-T., Kao, S.-J., Tsai,
9 F., Candice Lung, S.-C., Lin, F.-J., Lin, I. I., Hung, C.-C., and Tseng, C.-M.:
10 Sources, solubility, and dry deposition of aerosol trace elements over the East
11 China Sea, *Mar. Chem.*, 120, 116–127, doi:10.1016/j.marchem.2008.10.003, 2010b
- 12 Hsu, S. C., Lee, C. S. L., Huh, C. A., Shaheen, R., Lin, F. J., Liu, S. C., Liang, M. C.,
13 and Tao, J.: Ammonium deficiency caused by heterogeneous reactions during a
14 super Asian dust episode, *J. Geophys. Res.-Atmos.*, 119, 6803–6817, 2014.
- 15 Husar, R. B., Tratt, D., Schichtel, B. A., Falke, S., Li, F., Jaffe, D., Gasso, S., Gill, T.,
16 Laulainen, N. S., and Lu, F.: Asian dust events of April 1998, *J. Geophys.
Res.-Atmos.*, 106, 18317–18330, 2001.
- 18 Jickells, T., Kelly, S., Baker, A., Biswas, K., Dennis, P., Spokes, L., Witt, M., and
19 Yeatman, S.: Isotopic evidence for a marine ammonia source, *Geophys. Res. Lett.*,
20 30, 1374, doi:10.1029/2002GL016728, 2003.
- 21 Jickells, T., An, Z., Andersen, K. K., Baker, A., Bergametti, G., Brooks, N., Cao, J.,
22 Boyd, P., Duce, R., and Hunter, K.: Global iron connections between desert dust,
23 ocean biogeochemistry, and climate, *Science*, 308, 67–71, doi:10.1126/science.
24 1105959, 2005.
- 25 Jickells, T., Baker, A., Cape, J., Cornell, S., and Nemitz, E.: The cycling of organic
26 nitrogen through the atmosphere, *Philos. T. R. Soc. B*, 368, 20130115, doi:10.1098/
27 rstb.2013.0115, 2013.

- 1 Jung, J., Furutani, H., and Uematsu, M.: Atmospheric inorganic nitrogen in marine
2 aerosol and precipitation and its deposition to the North and South Pacific Oceans,
3 *J. Atmos. Chem.*, 68, 157–181, doi:10.1007/s10874-012-9218-5, 2011.
- 4 Jung, J., Furutani, H., Uematsu, M., Kim, S., and Yoon, S.: Atmospheric inorganic
5 nitrogen input via dry, wet, and sea fog deposition to the subarctic western North
6 Pacific Ocean, *Atmos. Chem. Phys.*, 13, 411–428, doi:10.5194/acp-13-411-2013,
7 2013.
- 8 Kanakidou, M., Duce, R. A., Prospero, J. M., Baker, A. R., Benitez-Nelson, C.,
9 Dentener, F. J., Hunter, K. A., Liss, P. S., Mahowald, N., and Okin, G. S.:
10 Atmospheric fluxes of organic N and P to the global ocean, *Global Biogeochem.*
11 Cy., 26, GB3026, doi:10.1029/2011GB004277, 2012.
- 12 Kang, C.-H., Kim, W.-H., Ko, H.-J., and Hong, S.-B.: Asian dust effects on total
13 suspended particulate (TSP) compositions at Gosan in Jeju Island, Korea, *Atmos.*
14 *Res.*, 94, 345–355, 2009.
- 15 Kang, J., Cho, B. C., and Lee, C.-B.: Atmospheric transport of water-soluble ions
16 (NO_3^- , NH_4^+ and nss- SO_4^{2-}) to the southern East Sea (Sea of Japan), *Sci. Total*
17 *Environ.*, 408, 2369–2377, 2010.
- 18 Kerminen, V.-M., Hillamo, R., Teinilä, K., Pakkanen, T., Allegrini, I., and Sparapani,
19 R.: Ion balances of size-resolved tropospheric aerosol samples: implications for the
20 acidity and atmospheric processing of aerosols, *Atmos. Environ.*, 35, 5255–5265,
21 2001.
- 22 Kim, I.-N., Lee, K., Gruber, N., Karl, D. M., Bullister, J. L., Yang, S., and Kim, T.-W.:
23 Increasing anthropogenic nitrogen in the North Pacific Ocean, *Science*, 346, 1102–
24 1106, 2014.
- 25 Kim, T.-W., Lee, K., Najjar, R. G., Jeong, H.-D., and Jeong, H. J.: Increasing N
26 abundance in the northwestern Pacific Ocean due to atmospheric nitrogen
27 deposition, *Science*, 334, 505–509, 2011.

- 1 Knapp, A. N., Sigman, D. M., and Lipschultz, F.: N isotopic composition of dissolved
2 organic nitrogen and nitrate at the Bermuda Atlantic Time-series Study site, Global
3 Biogeochem. Cy., 19, GB1018, doi:10.1029/2004GB002320, 2005.
- 4 Knapp, A. N., Sigman, D. M., Lipschultz, F., Kustka, A. B., and Capone, D. G.:
5 Interbasin isotopic correspondence between upper-ocean bulk DON and subsurface
6 nitrate and its implications for marine nitrogen cycling, Global Biogeochem. Cy.,
7 25, GB4004, doi:10.1029/2010GB003878, 2011.
- 8 Kundu, S., Kawamura, K., and Lee, M.: Seasonal variation of the concentrations of
9 nitrogenous species and their nitrogen isotopic ratios in aerosols at Gosan, Jeju
10 Island: implications for atmospheric processing and source changes of aerosols, J.
11 Geophys. Res.-Atmos., 115, D20305, doi:10.1029/2009JD013323, 2010.
- 12 Lange, C. A., Matschullat, J., Zimmermann, F., Sterzik, G., and Wienhaus, O.: Fog
13 frequency and chemical composition of fog water—a relevant contribution to
14 atmospheric deposition in the eastern Erzgebirge, Germany, Atmos. Environ., 37,
15 3731–3739, 2003.
- 16 Lesworth, T., Baker, A. R., and Jickells, T.: Aerosol organic nitrogen over the remote
17 Atlantic Ocean, Atmos. Environ., 44, 1887–1893, 2010.
- 18 Li, X. A., Yu, Z., Song, X., Cao, X., and Yuan, Y.: Nitrogen and phosphorus budgets
19 of the Changjiang River estuary, Chin. J. Oceanol. Limn., 29, 762–774, 2011.
- 20 Liang, J. Y., Horowitz, L. W., Jacob, D. J., Wang, Y., Fiore, A.M., Logan, J. A.,
21 Gardner, G. M., and Munger, J. W.: Seasonal budgets of reactive nitrogen species
22 and ozone over the United States, and export fluxes to the global atmosphere, J.
23 Geophys. Res.-Atmos., 103, 13435–13450, 1998.
- 24 Liu, X., Penner, J. E., and Herzog, M.: Global modeling of aerosol dynamics: model
25 description, evaluation, and interactions between sulfate and nonsulfate aerosols, J.
26 Geophys. Res.-Atmos., 110, D18206, doi:10.1029/2004JD005674, 2005.
- 27 Liu, X., Zhang, Y., Han, W., Tang, A., Shen, J., Cui, Z., Vitousek, P., Erisman, J. W.,

- 1 Goulding, K., Christie, P., Fangmeier, A., and Zhang, F.: Enhanced nitrogen
2 deposition over China, *Nature*, 494, 459–462, doi:10.1038/nature11917, 2013.
- 3 Mace, K. A., Duce, R. A., and Tindale, N.W.: Organic nitrogen in rain and aerosol at
4 Cape Grim, Tasmania, Australia, *J. Geophys. Res.-Atmos.*, 108, 4338, doi:10.1029/
5 2002JD003051, 2003a.
- 6 Mace, K. A., Kubilay, N., and Duce, R. A.: Organic nitrogen in rain and aerosol in the
7 eastern Mediterranean atmosphere: an association with atmospheric dust, *J.
8 Geophys. Res.-Atmos.*, 108, 4320, doi:10.1029/2002JD002997, 2003b.
- 9 Maria, S. F., and Russell, L. M.: Organic and inorganic aerosol below-cloud
10 scavenging by suburban New Jersey precipitation, *Environ. Sci. Technol.*, 39,
11 4793–4800, 2005.
- 12 Miyazaki, Y., Kawamura, K., Jung, J., Furutani, H., and Uematsu, M.: Latitudinal
13 distributions of organic nitrogen and organic carbon in marine aerosols over the
14 western North Pacific, *Atmos. Chem. and Phys.*, 11, 3037–3049,
15 doi:10.5194/acp-11-3037-2011, 2011.
- 16 Moore, K. F., Sherman, D. E., Reilly, J. E., Hannigan, M. P., Lee, T., and Collett, J. L.:
17 Drop size-dependent chemical composition of clouds and fogs. Part II: Relevance
18 to interpreting the aerosol/trace gas/fog system, *Atmos. Environ.*, 38, 1403–1415,
19 2004.
- 20 Nakamura, T., Matsumoto, K., and Uematsu, M.: Chemical characteristics of aerosols
21 transported from Asia to the East China Sea: an evaluation of anthropogenic
22 combined nitrogen deposition in autumn, *Atmos. Environ.*, 39, 1749–1758, 2005.
- 23 Nakamura, T., Ogawa, H., Maripi, D. K., and Uematsu, M.: Contribution of water
24 soluble organic nitrogen to total nitrogen in marine aerosols over the East China
25 Sea and western North Pacific, *Atmos. Environ.*, 40, 7259–7264, 2006.
- 26 Paulot, F., Jacob, D. J., Johnson, M. T., Bell, T. G., Baker, A. R., Keene, W. C., Lima,
27 I. D., Doney, S. C., and Stock, C. A.: Global oceanic emission of ammonia:

- 1 Constraints from seawater and atmospheric observations, Global Biogeochem. Cy.,
2 29, 1165–1178, doi:10.1002/2015GB005106, 2015.
- 3 Reis, S., Pinder, R. W., Zhang, M., Lijie, G., and Sutton, M. A.: Reactive nitrogen in
4 atmospheric emission inventories, Atmos. Chem. and Phys., 9, 7657–7677, doi:10.5
5 194/acp-9-7657-2009, 2009.
- 6 Safai, P., Kewat, S., Pandithurai, G., Praveen, P., Ali, K., Tiwari, S., Rao, P.,
7 Budhawant, K., Saha, S., and Devara, P.: Aerosol characteristics during winter fog
8 at Agra, North India, J. Atmos. Chem., 61, 101–118, 2008.
- 9 Sasakawa, M., and Uematsu, M.: Chemical composition of aerosol, sea fog, and
10 rainwater in the marine boundary layer of the northwestern North Pacific and its
11 marginal seas, J. Geophys. Res.-Atmos., 107, ACH 17-11-ACH 17-19, 2002.
- 12 Sasakawa, M., and Uematsu, M.: Relative contribution of chemical composition to
13 acidification of sea fog (stratus) over the northern North Pacific and its marginal
14 seas, Atmos. Environ., 39, 1357–1362, 2005.
- 15 Savoie, D., and Prospero, J.: Water-soluble potassium, calcium, and magnesium in the
16 aerosols over the tropical North Atlantic, J. Geophys. Res.-Oceans, 85, 385–392,
17 1980.
- 18 Shao, Y. and Dong, C.: A review on East Asian dust storm climate, modelling and
19 monitoring, Global Planet. Change, 52, 1–22, 2006.
- 20 Shi, G., Li, Y., Jiang, S., An, C., Ma, H., Sun, B., and Wang, Y.: Large-scale spatial
21 variability of major ions in the atmospheric wet deposition along the China
22 Antarctica transect (31 °N–69 °S), Tellus B, 64, 1–10, 2012.
- 23 Shi, J., Gao, H., Qi, J., Zhang, J., and Yao, X.: Sources, compositions, and
24 distributions of water-soluble organic nitrogen in aerosols over the China Sea, J.
25 Geophys. Res.-Atmos., 115, D17303, doi:10.1029/2009JD013238, 2010.
- 26 Spokes, L. J. and Liss, P. S.: Photochemically induced redox reactions in seawater, II.
27 Nitrogen and iodine, Mar. Chem., 54, 1–10, 1996.

- 1 Srinivas, B., Sarin, M., and Sarma, V.: Atmospheric dry deposition of inorganic and
2 organic nitrogen to the Bay of Bengal: impact of continental outflow, Mar. Chem.,
3 127, 170–179, 2011.
- 4 Sun, J., Zhang, M., and Liu, T.: Spatial and temporal characteristics of dust storms in
5 China and its surrounding regions, 1960–1999: Relations to source area and climate,
6 J. Geophys. Res.- Atmos., 106, 10325–10333, 2001.
- 7 Uematsu, M., Hattori, H., Nakamura, T., Narita, Y., Jung, J., Matsumoto, K.,
8 Nakaguchi, Y., and Kumar, M. D.: Atmospheric transport and deposition of
9 anthropogenic substances from the Asia to the East China Sea, Mar. Chem., 120,
10 108–115, 2010.
- 11 Violaki, K., Zarbas, P., and Mihalopoulos, N.: Long-term measurements of dissolved
12 organic nitrogen (DON) in atmospheric deposition in the Eastern Mediterranean:
13 fluxes, origin and biogeochemical implications, Mar. Chem., 120, 179–186, 2010.
- 14 Violaki, K., Sciare, J., Williams, J., Baker, A. R., Martino, M., and Mihalopoulos, N.:
15 Atmospheric water-soluble organic nitrogen (WSON) over marine environments: a
16 global perspective, Biogeosciences, 12, 3131–3140, doi:10.5194/bg-12-3131-2015,
17 2015.
- 18 Vione, D., Maurino, V., Minero, C., and Pelizzetti, E.: Reactions induced in natural
19 waters by irradiation of nitrate and nitrite ions, in: Environmental Photochemistry
20 Part II, Springer, 221–253, 2005.
- 21 Watanabe, K., Takebe, Y., Sode, N., Igarashi, Y., Takahashi, H., and Dokya, Y.: Fog
22 and rain water chemistry at Mt. Fuji: A case study during the September 2002
23 campaign, Atmos. Res., 82, 652–662, doi:10.1016/j.atmosres.2006.02.021, 2006.
- 24 Wedyan, M., Fandi, K., and Al-Rousan, S.: Bioavailability of atmospheric dissolved
25 organic nitrogen in the marine aerosol over the Gulf of Aqaba, Australian J. Basic
26 Appl. Sci., 1, 208–212, 2007.
- 27 Xie, H., Bélanger, S., Song, G., Benner, R., Taalba, A., Blais, M., Tremblay, J.-É., and

- 1 Babin, M.: Photoproduction of ammonium in the southeastern Beaufort Sea and its
2 biogeochemical implications, *Biogeosciences*, 9, 3047–3061, doi:10.5194/bg-9-
3 3047-2012, 2012.
- 4 Yan, G. and Kim, G.: Sources and fluxes of organic nitrogen in precipitation over the
5 southern East Sea/Sea of Japan, *Atmos. Chem. Phys.*, 15, 2761–2774, doi:10.5194
6 /acp-15-2761-2015, 2015.
- 7 Yao, X. H. and Zhang, L.: Supermicron modes of ammonium ions related to fog in
8 rural atmosphere, *Atmos. Chem. Phys.*, 12, 11165–11178, doi:10.5194/acp-12-
9 11165-2012, 2012.
- 10 Yue, Y., Niu, S., Zhao, L., Zhang, Y., and Xu, F.: Chemical Composition of Sea Fog
11 Water Along the South China Sea, *Pure Appl. Geophys.*, 169, 2231–2249, doi:10.
12 1007/s00024-012-0486-4, 2012.
- 13 Yue, Y., Niu, S., Zhao, L., Zhang, Y., and Xu, F.: The influences of macro-and
14 microphysical characteristics of sea-fog on fog-water chemical composition, *Adv.*
15 *Atmos. Sci.*, 31, 624–636, 2014.
- 16 Zamora, L., Prospero, J., and Hansell, D.: Organic nitrogen in aerosols and
17 precipitation at Barbados and Miami: Implications regarding sources, transport and
18 deposition to the western subtropical North Atlantic, *J. Geophys. Res.-Atmos.*, 116,
19 D20309, doi:10.1029/2011JD015660, 2011.
- 20 Zhang, G., Zhang, J., and Liu, S.: Characterization of nutrients in the atmospheric wet
21 and dry deposition observed at the two monitoring sites over Yellow Sea and East
22 China Sea, *J. Atmos. Chem.*, 57, 41–57, 2007.
- 23 Zhang, R., Jing, J., Tao, J., Hsu, S.-C., Wang, G., Cao, J., Lee, C., Zhu, L., Chen, Z.,
24 and Zhao, Y.: Chemical characterization and source apportionment of PM 2.5 in
25 Beijing: seasonal perspective, *Atmos. Chem. Phys.*, 13, 7053–7074, doi:10.5194/
26 acp-13-7053-2013, 2013.
- 27 Zhang, S.-P., Xie, S.-P., Liu, Q.-Y., Yang, Y.-Q., Wang, X.-G., and Ren, Z.-P.:

- 1 Seasonal variations of Yellow Sea fog: observations and Mechanisms*, J. Climate,
2 22, 6758–6772, doi:10.1175/2009jcli2806.1, 2009.
- 3 Zhang, Y., Song, L., Liu, X., Li, W., Lü, S., Zheng, L., Bai, Z., Cai, G., and Zhang, F.:
4 Atmospheric organic nitrogen deposition in China, Atmos. Environ., 46, 195–204,
5 2012.
- 6 Zhu, L., Chen, Y., Guo, L., and Wang, F.: Estimate of dry deposition fluxes of
7 nutrients over the East China Sea: the implication of aerosol ammonium to
8 non-sea-salt sulfate ratio to nutrient deposition of coastal oceans, Atmos. Environ.,
9 69, 131–138, doi:10.1016/j.atmosenv.2012.12.028, 2013.

1 Table 1. Nitrogen speciation in various aerosols reported from different regions.

Sample type	Date	Location	NO_3^-	NH_4^+	WSON	NO_3^-	NH_4^+	WSON	Reference	
			nmol m ⁻³	nmol m ⁻³	nmol m ⁻³	% ^a	% ^a	% ^a		
TSP (Sea fog)	Mar–Apr 2014	ECSs	Shelf	536 ± 300	442 ± 194	147 ± 171	48 ± 7	42 ± 9	10 ± 6	This study
TSP (Dust)	Mar–Apr 2014	NWPO	Remote ocean	100 ± 23	138 ± 24	11.2 ± 4.0	41 ± 5	56 ± 7	5 ± 2	This study
TSP (Bgd.)	Mar–Apr 2014	NWPO	Remote ocean	26 ± 32	54 ± 45	10.9 ± 6.8	27 ± 9	60 ± 11	14 ± 8	This study
TSP (Dust)	Aug–Sep 2007, 2008	Barbados, Atlantic	Island	101 ± 4	11 ± 7	1.4 ± 1.3	45 ^c	49 ^c	6 ^c	Zamora et al. (2011)
TSP (Dust)	May 2007–July 2009	Miami, FL, Atlantic	Coast city	28 ± 9	26 ± 10	3.0 ± 2.0	50 ^c	45 ^c	5 ^c	
PM _{>2} (Dust)		Tropic Atlantic Ocean						14	Violaki et al. (2015)	
TSP (Dust)	Mar 2005–Apr 2007	Southwest ECS	Shelf	84 ± 98	177 ± 151	—	—	—	—	Hsu et al. (2010b)
TSP (Dust)	Feb 1992–May 2004	Island of Jeju	Island	71 ± 44	72 ± 48	—	—	—	—	Kang et al. (2009)
TSP	Feb–Mar 2007	Northwest ECS	Shelf	68 ^c	193 ^c	—	—	—	—	Shi et al. (2010)
TSP	Mar 2005–Apr 2007	Southwest ECS	Shelf	38 ± 45	89 ± 76	—	—	—	—	Hsu et al. (2010b)
TSP	Sep–Oct 2002	ECS	Shelf	34 ^c	136 ^c	54 ± 36	15 ^c	61 ^c	24	Nakamura et al. (2006)
TSP	Mar 2004	ECS	Shelf	39 ^c	91 ^c	16 ± 19	27 ^c	62 ^c	10	
TSP	Mar 2005, Apr 2006	Yellow Sea	Shelf	—	—	—	—	—	20	Shi et al. (2010)
TSP	Apr 2010	Northwest ECS	Island	111 ^c	76 ^c	—	—	—	—	Zhu et al. (2013)
TSP	Mar 2011	Northwest ECS	Island	137 ^c	202 ^c	—	—	—	—	Zhu et al. (2013)
TSP	Spring 2003–2004	Northeast ECS	Island	85 ± 47 ^c	133 ± 78 ^c	—	—	—	—	Kundu et al. (2010)
TSP	Jul–Aug 2008	NWPO	Remote ocean	2.5	5.6	—	—	—	—	Jung et al. (2013)
TSP	Aug 2003–Sep 2005	Gulf of Aqaba	Coast	39 ± 19	25 ± 14	8 ± 5	53 ^c	34 ^c	11 ^c	Chen et al. (2007)
TSP	Nov–Dec 2000	Island of Tasmania	Island	11 ± 7	2.6 ± 3.0	3.6 ± 5.7	63	15	21	Mace et al. (2003a)
TSP	Aug–Sep 2008	NWP	Remote ocean	1.8 ± 1.5	1.2 ± 1.1	1.1 ± 0.93	43 ^c	30 ^c	28 ^c	Miyazaki et al. (2011)
TSP	Apr 2007–Mar 2008	Marina, Singapore	urban	50 ± 31	14 ± 8	56 ± 22	40 ± 15	11 ± 6	49 ± 17	He et al. (2011)
TSP	Jan–Dec 2006	Keelung, Taiwan	Coast city			76 ± 28		26 ^c	Chen et al. (2010)	

TSP (Sea-spray)				6.7 ± 2.7	4.2 ± 1.7	0.5 ± 0.3	59 ^c	37 ^c	4 ^c	Zamora et al. (2011)
TSP (Bb) ^b				11 ± 11	18 ± 13	3.3 ± 2.0	34 ^c	56 ^c	10 ^c	
TSP (Bb) ^b				28 ± 16	48 ± 48	6.2 ± 6.4	34 ^c	58 ^c	8 ^c	Zamora et al. (2011)
TSP (Pollution)				22 ± 11	23 ± 24	3.7 ± 2.8	45 ^c	48 ^c	8 ^c	
PM _{1.3-10}	2005, 2006	Crete, Greece	Island	26 ± 9	8.9 ± 4.0	5.5 ± 3.9	64	23	13	Violaki et al. (2010)
PM _{1.3}	2005, 2006	Crete, Greece		1.5 ± 1.3	70 ± 35	12 ± 14	2	85	13	
PM _{2.5}	Jan-Dec 2005	Indian Ocean	Remote ocean	0.3 ± 0.2	1.3 ± 1.0	0.8 ± 1.4	14	53	32	Violaki et al. (2015)
PM _{2.5-10}				0.2 ± 0.1	0.3 ± 0.1	0.2 ± 0.4	26	39	35	
PM _{2.5}	Jan 2007	Middle S. Atlantic	Remote ocean			1.3 ± 0.8			51	

1 ^aPercentage in total dissolved nitrogen

2 ^bBb indicated Biomass burning

3 ^cCalculated value from the original data

1 Table 2. Mean molar concentrations (nmol m^{-3}) of major ionic species together with
 2 Al (ng m^{-3}) in sea fog modified aerosols and dust aerosols in the ECSs.

	Sea fog ^a mean \pm SD	Dust ^b mean \pm SD	Dust ^c mean \pm SD
Na^+	123.2 ± 97.5	294.8 ± 238.3	130.4 ± 85.2
NH_4^+	441.5 ± 193.9	177.6 ± 150.7	72.2 ± 47.7
Mg^{2+}	24.1 ± 16.5	41.2 ± 32.4	25.0 ± 12.9
K^+	17.5 ± 9.9	21.8 ± 19.1	17.9 ± 9.2
Ca^{2+}	54.7 ± 52.2	61.7 ± 39.5	76.9 ± 58.5
Cl^-	125.2 ± 111.3	280.9 ± 349.1	121.3 ± 101.6
NO_3^-	535.9 ± 299.7	83.6 ± 98.4	71.0 ± 43.5
SO_4^{2-}	172.5 ± 54.1	145.2 ± 103.2	104.0 ± 47.2
nss- SO_4^{2-}	165.1 ± 50.3	94.9 ± 89.0	96.1 ± 47.3
Total Al	2460 ± 2160	3470 ± 2730	4900 ± 6500
Soluble Al	124 ± 36	38 ± 45	nd.
Al Solubility	$5.0 \pm 1.7\%$	$1.1 \pm 1.6\%$	nd.
Relative acidity	0.73 ± 0.13	1.07	1.06

3 ^aThis study; ^bHsu et al. (2010b); ^cKang et al. (2009); nd.: no data

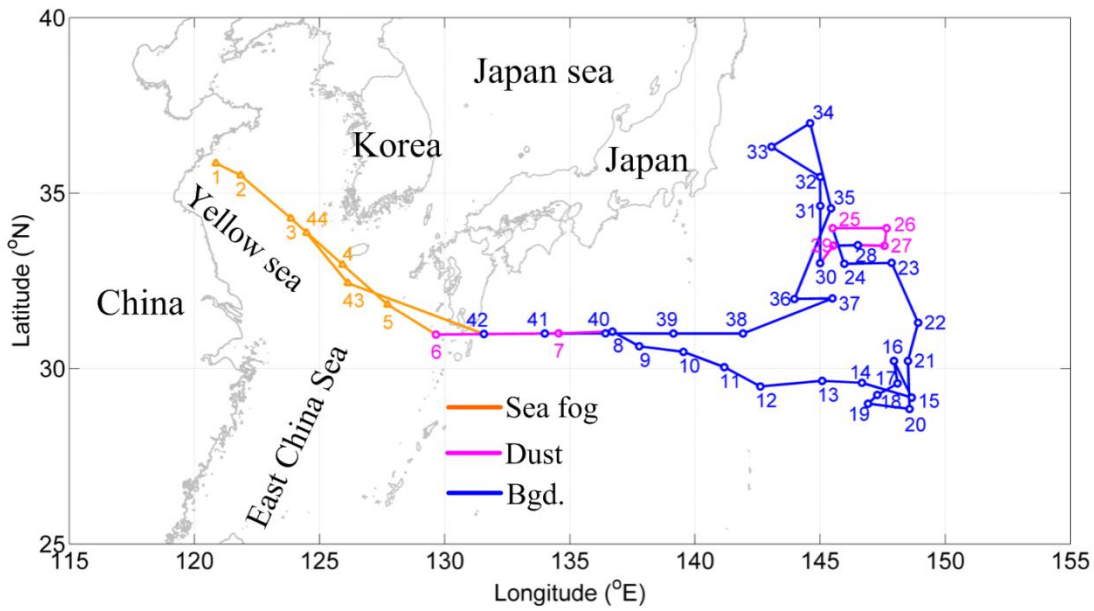
4

1 Table 3. The depositional fluxes reported or calculated for the Asian region and Pacific Ocean based on assumed deposition velocity.

Locations	Collection type	Date	NO_3^- ^a	NH_4^+ ^a	WSO ^a	Total ^a	Reference
ECSs (Sea fog)	Cruise	Mar-Apr 2014	926 ± 518	38 ± 17	127 ± 148	1090 ± 671	This study
NWPO (Dust)	Cruise	Mar-Apr 2014	172 ± 40	11.9 ± 2.1	6.5 ± 5.7	190 ± 41.6	This study
NWPO (Bgd.)	Cruise	Mar-Apr 2014	44.6 ± 55.3	4.66 ± 3.90	7.6 ± 6.5	56.8 ± 59.1	This study
Subarctic western	Cruise	Jul-Aug 2008	3.3 ± 2.3	1.9 ± 0.63	--	5.3 ± 2.6	Jung et al. (2011)
North Pacific							
Subtropical western	Cruise	Aug-Sep 2008	3.0 ± 1.5	2.7 ± 2.1	--	5.7 ± 3.5	Jung et al. (2011)
North Pacific							
Central North Pacific	Cruise	Jan 2009	1.6 ± 0.44	1.4 ± 0.96	--	3.1 ± 1.4	Jung et al. (2011)
Northwest ECS*	Cruise	Feb-Mar 2007	117	17	--	134	Shi et al.(2010)
Southwest ECS*	Cruise	Spring 2005-2007	66	8	--	74	Hsu et al. (2010b)
Northwest ECS*	Coastal island	Apr 2010	192	6.6	--	198.6	Zhu et al. (2013)
Northwest ECS*	Coastal island	Mar 2011	237	17.5	--	254.5	Zhu et al. (2013)

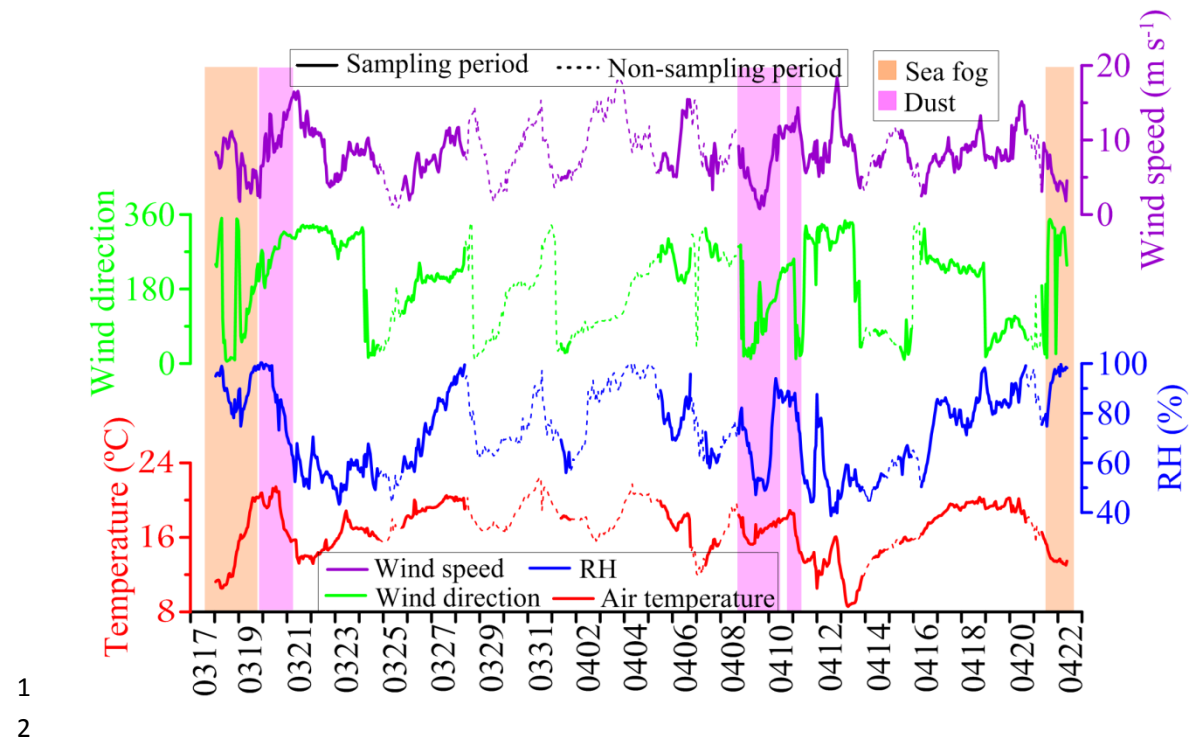
2 * recalculated fluxes based on assumed deposition velocity

3 ^a in $\mu\text{mol N m}^{-2} \text{ d}^{-1}$

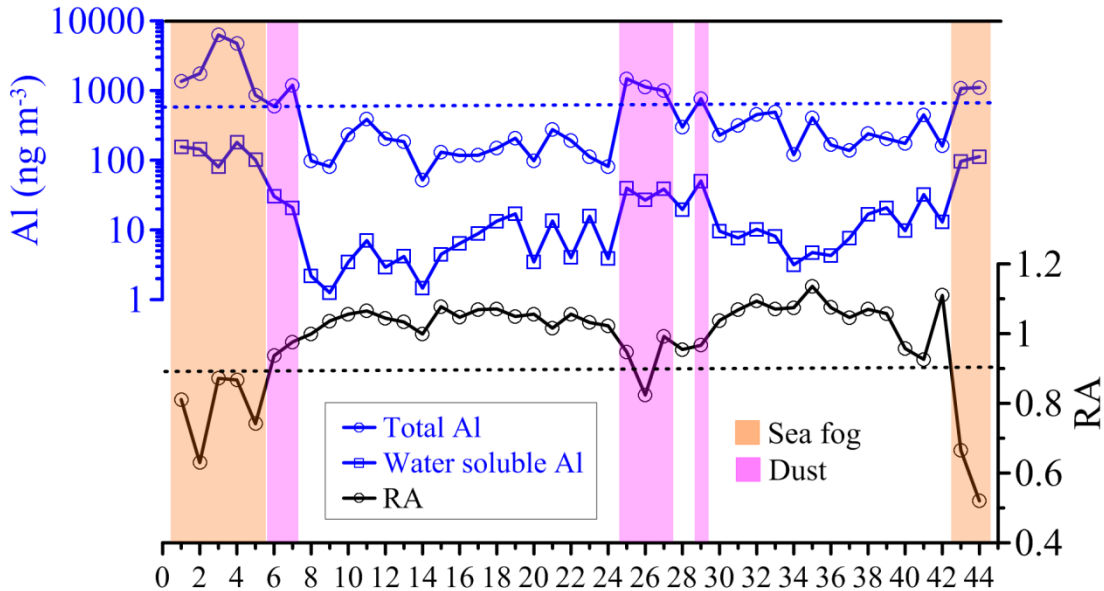


1
2

3 Figure 1. Map of the cruise track. Orange, pink and blue indicate sea fog, dust and
4 background days during the cruise. Sample number and the collection range were
5 shown.



1 Figure 2. The meteorological parameters collected during the sampling period (solid
2 line). Wind speed is in purple, wind direction in green, RH in blue and temperature in
3 red. The orange shadings indicate the period of sea fog contact and pink indicate the
4 dust period. Non-sampling period is in dashed curves.
5
6



2
3 Figure 3. Total and water soluble Al concentrations and relative acidity (RA) for TSP.
4 The orange bars indicate the sea fog period, the pink bars indicate the dust period.
5 Sample identifications are shown on the x-axis (see Table S1). The horizontal blue
6 dashed line (590 ng m^{-3}) stands for the reference to define background aerosols, and
7 black dashed line indicates the criterion of 0.9 for relative acidity.

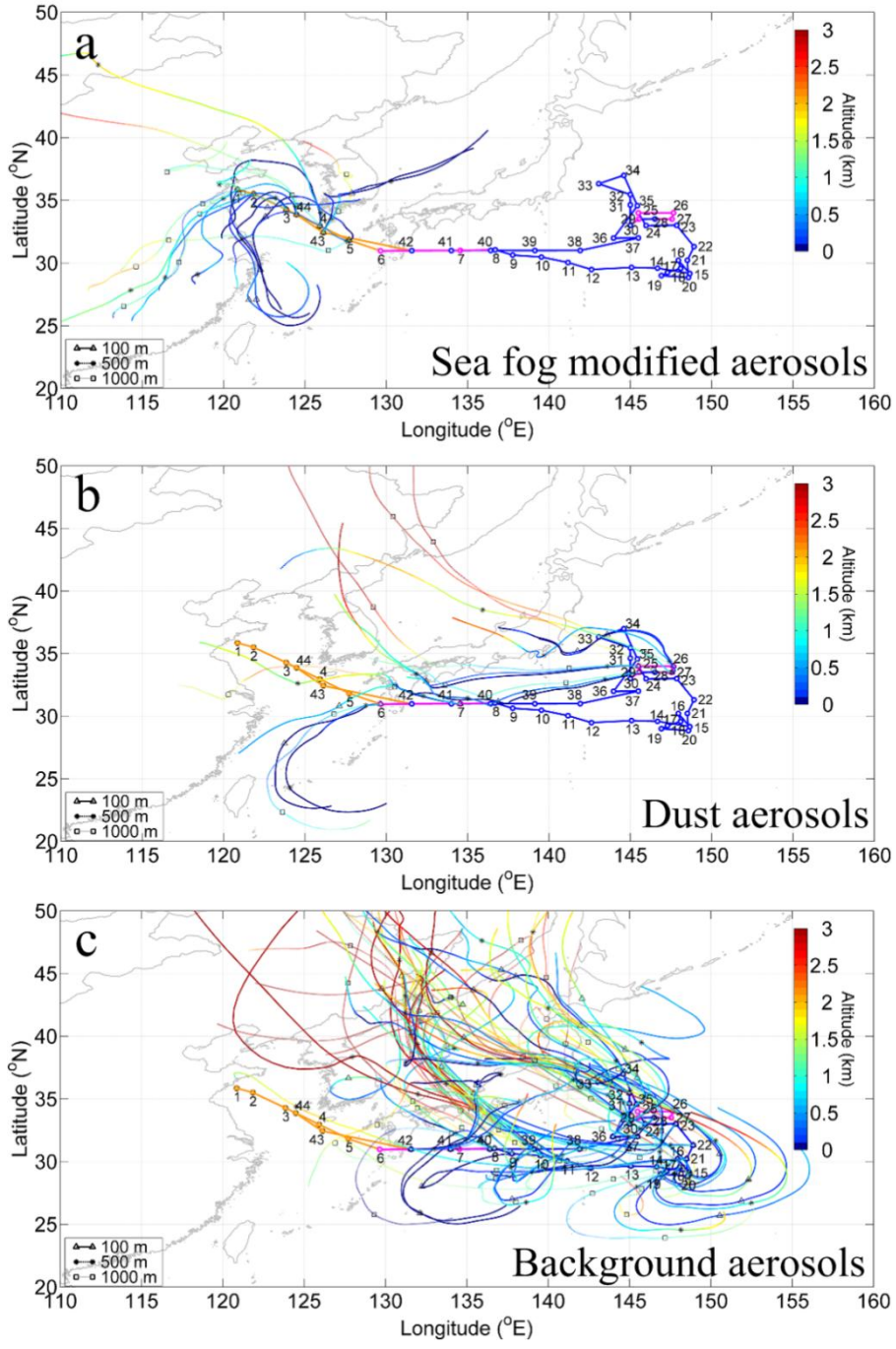


Figure 4. Map and cruise track superimposed on 3-days air mass backward trajectories corresponding to each sample. Altitudes of 100 m a.s.l. (triangles), 500 m a.s.l. (asterisks) and 1000 m a.s.l. (squares) are above sea levels during the collecteion of (a) sea fog modified aerosols, (b) dust aerosols and (c) background aerosols. The colour bar represents the altitude (in km).

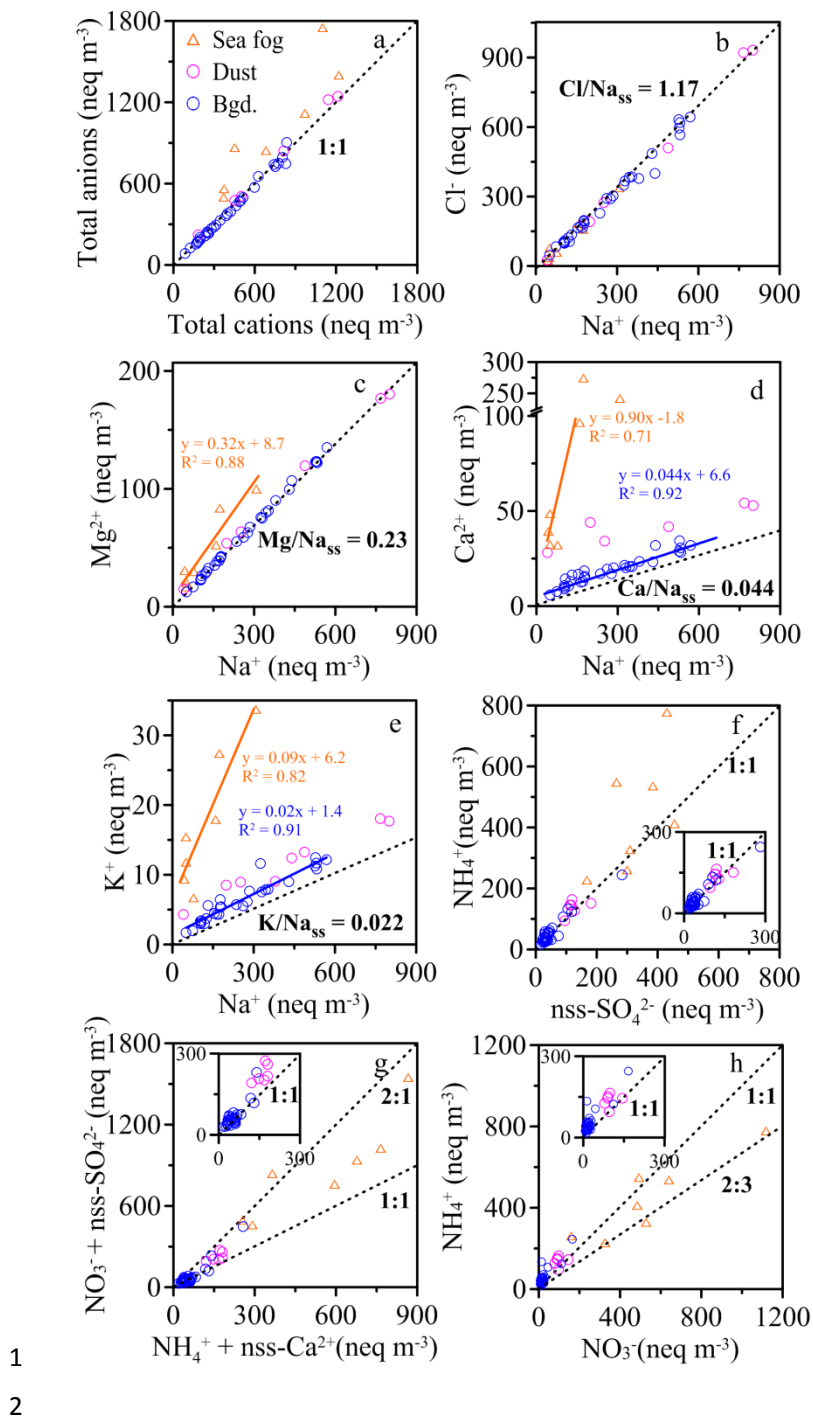


Figure 5. Scatter plots for equivalent concentrations of specific ions. (a) total anions vs. total cations, (b) chloride vs. sodium, (c) magnesium vs. sodium, (d) calcium vs. sodium, (e) potassium vs. sodium, (f) ammonium vs. nss-sulfate, (g) Σ (nitrate + nss-sulfate) vs. Σ (nss-calcium + ammonium) and (h) nitrate vs. ammonium. Orange, pink and blue are for sea fog modified, dust and background aerosols.

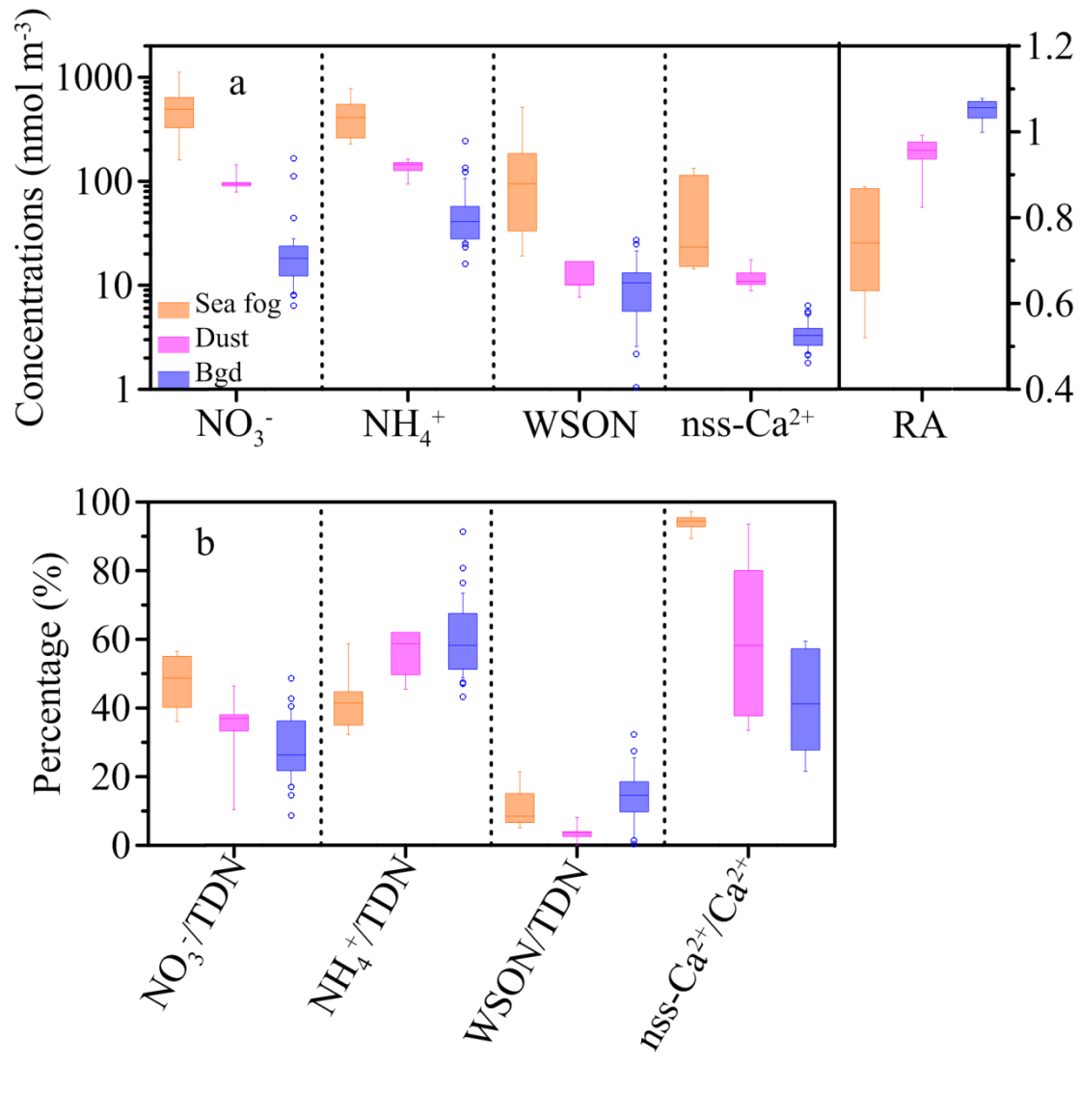
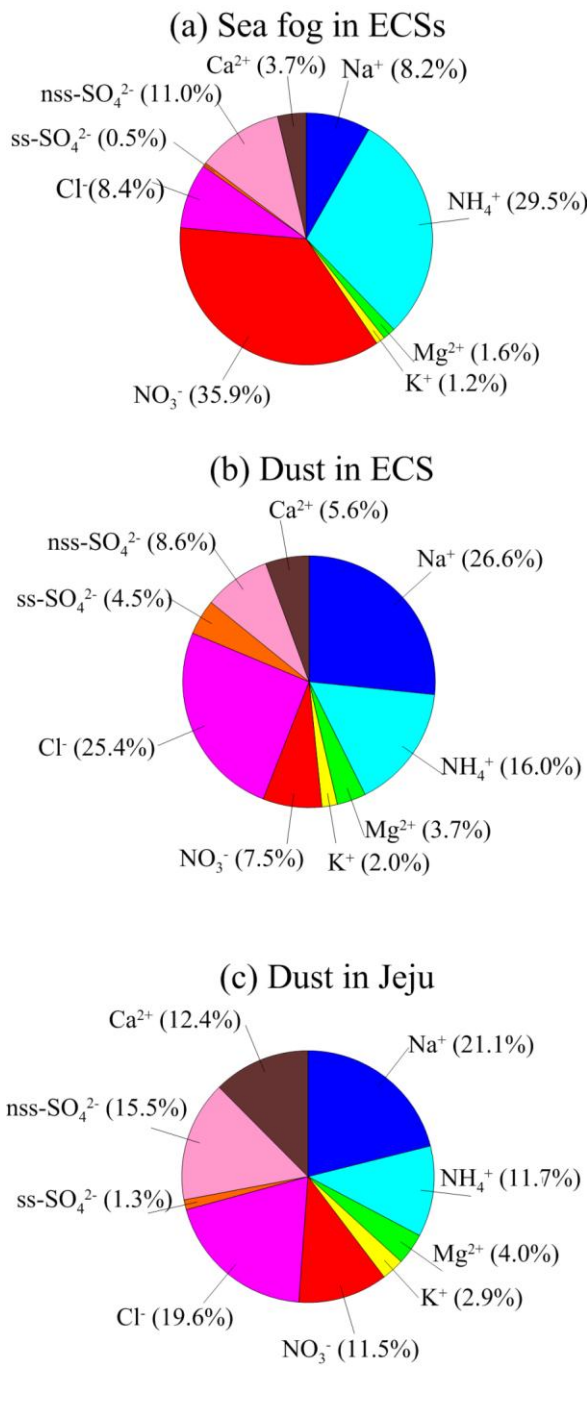


Figure 6. Box plots for (a) concentrations of NO₃⁻, NH₄⁺, WSON and nss-Ca²⁺, and RA, and (b) fractions of nitrogen species in total dissolved nitrogen and proportion of nss-Ca²⁺ in Ca²⁺, in sea fog modified, dust and background aerosols. The large boxes represent the inter-quartile range from the 25th to 75th percentile. The line inside the box indicates the median value. The whiskers extend upward to the 90th and downward to the 10th percentile.



3 Figure 7. Pie charts of ion distribution for (a) sea fog modified aerosols (this study),
4 (b) dust aerosols collected over the East China Sea ($n = 8$) (Hsu et al., 2010b), and (c)
5 dust aerosols collected on the island of Jeju ($n = 49$) (Kang et al., 2009).|

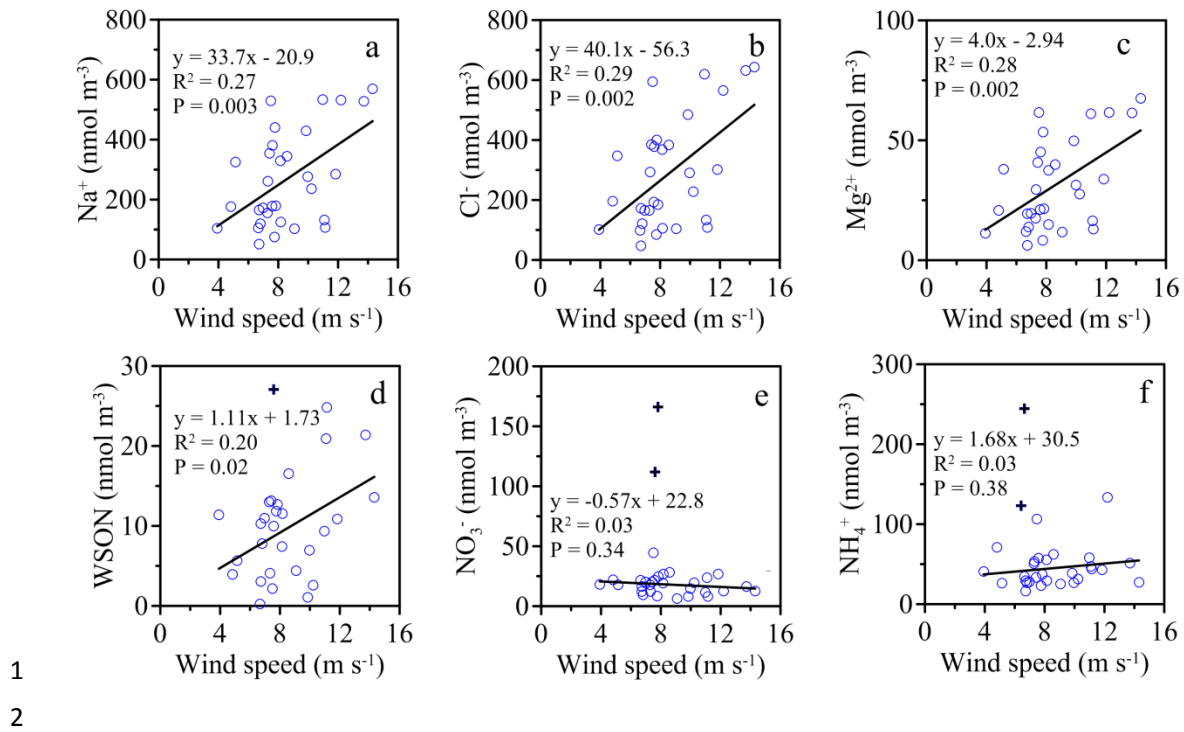


Figure 8. Scatter plots of concentrations of (a) Na^+ , (b) Cl^- , (c) Mg^{2+} , (d) WSON, (e) NO_3^- , and (f) NH_4^+ against corresponding wind speed for background aerosols. Wind speed was derived by averaging wind speed (5 min average) in corresponding sampling intervals. Crosses in (d), (e) and (f) were not considered during the linear regression.

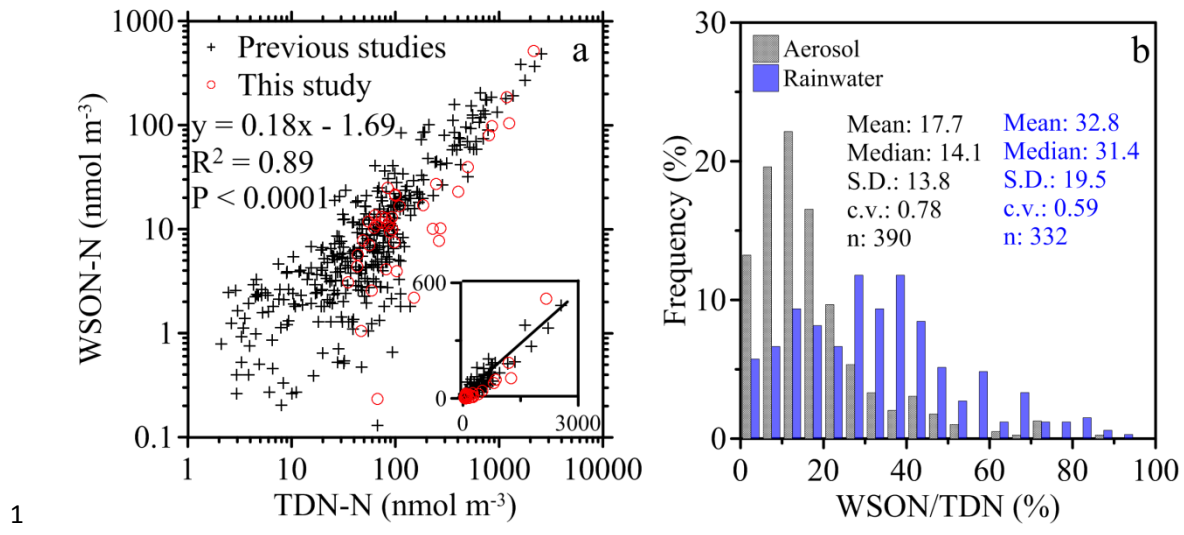


Figure 9. (a) Scatter plot of published aerosol WSON and TDN concentrations from the world (red circles for this study, black crosses from Lesworth et al., 2010; Chen et al., 2007; Mace et al., 2003; Miyazaki et al., 2011; Shi et al., 2010; Srinivas et al., 2011; Zamora et al., 2011; and Violaki et al., 2015). (b) Frequency histograms for percentage WSON in aerosol TDN (grey bars, data from Fig. 9a) and in rainwater (blue bars, data from Cornell, 2011; Zhang et al., 2012; Altieri et al., 2012; Cui et al., 2014; Chen et al., 2015; and Yan and Kim, 2015).

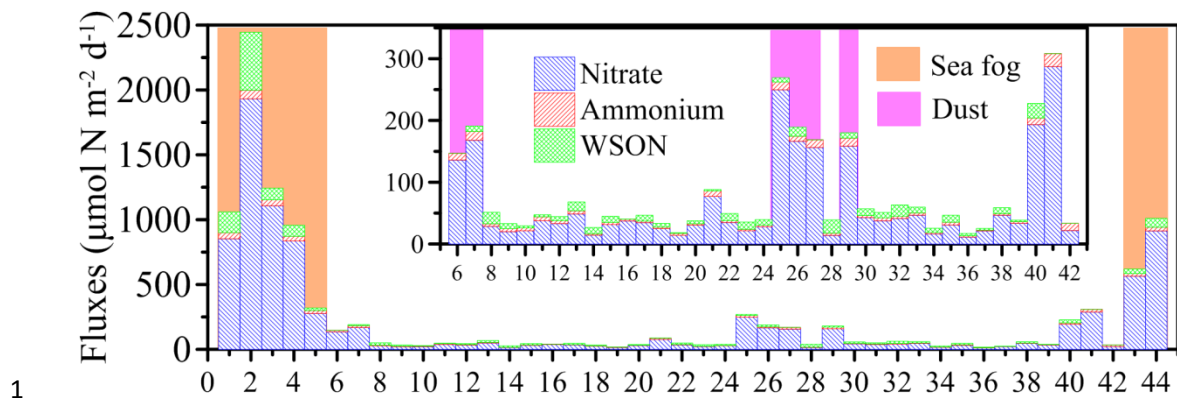


Figure 10. Dry deposition of aerosol nitrogen against sample identification. Nitrate is in blue, ammonium in red and WSON in green. Sample identifications, which matched with Table S1, are shown on the x axis.